Psychology of Aesthetics, Creativity, and the Arts

Neuroarchitecture of Aesthetic Experience: Investigating Brain Oscillations for Interior Spaces With Curved Boundaries in Virtual Reality

Tugce Elver Boz, Ismail Hakkı Bayer, Seyda Evsen, Halime Demirkan, and Burcu A. Urgen

Online First Publication, September 29, 2025. https://dx.doi.org/10.1037/aca0000812

AMERICAN PSYCHOLOGICAL ASSOCIATION
DIVISION 10
Psychology of Aesthetics, Creativity, and the Arts

ISSN: 1931-3896
https://doi.org/10.1037/aca0000812

Neuroarchitecture of Aesthetic Experience: Investigating Brain Oscillations for Interior Spaces With Curved Boundaries in Virtual Reality

Tugce Elver Boz[1], Ismail Hakkı Bayer[2, 3], Seyda Evsen[4], Halime Demirkan[1], and Burcu A. Urgen[3, 4, 5]
[1] Department of Interior Architecture and Environmental Design, Faculty of Art, Design and Architecture, I.D. Bilkent University
[2] Faculty of Psychology and Neuroscience, Maastricht University
[3] Department of Psychology, Faculty of Economics, Administrative and Social Sciences, I.D. Bilkent University
[4] Interdisciplinary Neuroscience Graduate Program, Graduate School of Science and Engineering, I.D. Bilkent University
[5] Aysel Sabuncu Brain Research Center and National Magnetic Resonance Research Center (UMRAM), I.D. Bilkent University

This study takes an interdisciplinary approach to investigate interior space perception—environments where people spend much of their daily lives—by examining behavior and brain activity. Integrating psychology, neuroscience, and architecture, it explores three key components of aesthetic experience (familiarity, excitement, and fascination) within virtual reality environments. Using 32 virtual interior spaces with curved boundary types and varying architectural variables (size, light, texture, and color), 20 participants assessed aesthetic qualities while their brain activity was recorded via electroencephalography. Behavioral results reveal that horizontal boundaries were perceived as more familiar, whereas vertical boundaries (VB) evoked higher levels of excitement and fascination. Neural results showed that alpha and beta oscillations reflected perceptual and emotional engagement, particularly under vertical boundaries. Alpha desynchronization was observed in posterior and right-hemisphere regions, suggesting enhanced attentional engagement and spatial analysis during VB-related judgments. Beta activity showed differentiated patterns: Desynchronization during familiarity under VB reflected active environmental evaluation, whereas synchronization during fascination under VB pointed to top-down processing and emotional resonance. Notably, theta synchronization increased during familiarity judgments under VB, aligning with its role in memory encoding and cognitive effort. Together, these findings demonstrate that architectural features systematically modulate both the subjective experience and the neural dynamics of aesthetic evaluation. This study contributes to neuroarchitecture by elucidating how architectural design influences aesthetic experiences, offering insights for creating more functional and emotionally resonant spaces.

Keywords: aesthetic experience, electroencephalography, neuroarchitecture, neuroaesthetics, virtual reality

The intersection between neuroscience and architecture is an emerging multidisciplinary field that seeks to understand the complex relationship between the built environment and human experience. Historically, architecture has been concerned with space's aesthetic, functional, and structural aspects, while neuroscience has focused on the brain's functioning. Integrating neuroscience into architectural practice—neuroarchitecture—provides a scientific basis for understanding how people perceive, interact with, and are emotionally affected by their physical environment (Eberhard, 2009). Using the tools and methods of cognitive science, such as neuroimaging, researchers have begun to uncover how different architectural designs can stimulate specific neural responses, affecting emotions, cognition, and behavior.

Since the 1960s, attempts to integrate architecture with cognitive science, particularly in environmental behavior and spatial analysis, have paved the way for current efforts to integrate neuroscience into architectural research (Lee et al., 2022). These efforts seek to explain how architectural elements such as space, form, light, and texture affect brain function and offer valuable insights into how the built environment can enhance human well-being. Neuroarchitecture thus represents a promising way to create aesthetically pleasing spaces and optimized for cognitive and emotional health.

This study explores the neuroscience of architecture, focusing on the relationship between aesthetic judgments, architectural variables, and neural oscillations. By examining how aesthetic judgments and how various architectural variables with curved boundary types affect brain oscillations, this study aims to deepen human understanding of how the built environment can be designed to promote comfort and engagement.

Literature Review

Neuroarchitecture and Aesthetics

Neuroarchitecture, combining neuroscience and architecture, is an emerging multidisciplinary field. It offers new insights into the

Dirk B. Walther served as action editor.
Tugce Elver Boz https://orcid.org/0000-0001-6614-2288
The present study is supported by TÜBİTAK grant awarded to Tugce Elver Boz, Halime Demirkan, and Burcu A. Urgen. The authors would like to thank Elif Ahsen Cakmakci for help with preprocessing the electroencephalography data. The authors declare that they have no conflicts of interest.
Correspondence concerning this article should be addressed to Tugce Elver Boz, Department of Interior Architecture and Environmental Design, Faculty of Art, Design and Architecture, I.D. Bilkent University, 06800 Bilkent, Ankara, Turkey. Email: tugce.elver@bilkent.edu.tr

experiential design components traditionally overlooked in architecture. Incorporating neuroimaging methods along with behavioral and experiential paradigms, "neuroscience of architecture" serves as an empirical foundation for understanding how architecture influences behavior and the brain (Dobkins & Heyman, 2013; Dzebic et al., 2013; Jelić et al., 2016; Martínez-Soto et al., 2013; Nanda et al., 2013)

Recent studies have demonstrated the potential of neuroarchitecture to improve the understanding of aesthetic experiences in architecture. For example, the emerging field of neuroaesthetics explores the neural basis of aesthetic judgments and reveals how they can evoke associated neural responses (Vartanian et al., 2013, 2015). Furthermore, neuroimaging technologies such as electroencephalography (EEG) and functional magnetic resonance imaging (fMRI) have been used to study how different architectural stimuli affect brain activity, shedding light on the neural processes underlying spatial perception and decision making.

The field draws heavily from neuroaesthetics, which investigates the neural foundations of aesthetic perception, which gained significant empirical and theoretical traction in the 2000s. Some researchers identify 2004 as the formal emergence of neuroaesthetics, marked with the publication of key neuroimaging studies that explored the neural correlates of aesthetic experiences (e.g., Cela-Conde et al., 2004; Kawabata & Zeki, 2004; Vartanian & Goel, 2004). These studies established neuroaesthetics as a scientific field, showing that the responses to beauty and preferences are linked to specific brain processes. Together, they transformed the way researchers approach aesthetics, shifting the focus from a philosophical concept to one grounded in brain function.

The study of aesthetics in the built environment focuses on understanding the neural basis of how people evaluate architecture (Eberhard, 2009). Some of the earliest research in this field used fMRI to investigate neural responses to artworks and to analyze the mechanisms in brain to contribute to aesthetic experiences (Chatterjee, 2004a, 2004b). Subsequently, researchers developed foundational models outlining the cognitive and neural systems involved in aesthetic judgments (Chatterjee & Vartanian, 2014; Leder et al., 2004). Leder et al. (2004) proposed a stage model of aesthetic appreciation that partitions the process into five stages: perceptual analysis, implicit memory integration, explicit classification, cognitive mastering, and evaluative judgment. This model attends to the ways in which bottom-up perceptual features and top-down cognitive processes are involved in aesthetic contexts. Expanding on this, Chatterjee and Vartanian (2014) identified specific neural systems underlying aesthetic judgement, including the sensory cortices, attentional network and centers implicated in emotion, such as the orbitofrontal cortex (OFC) and anterior cingulate cortex. Together, these models provide a more integrated view of how people perceive, interpret, and emotionally respond to architectural cues.

Albeit a useful tool to pinpoint brain areas involved in aesthetic judgments, the utilization of fMRI limited the scope of aesthetic research in neuroarchitecture since incorporating a virtual environment (VE) was not feasible because of technical issues (Coburn et al., 2020). One limitation of early fMRI studies is their reliance on two-dimensional stimuli, as the technology constraints movement, preventing the exploration of three-dimensional environments. Coburn et al. (2020) acknowledged this as a limitation, emphasizing the potential of using more immersive technologies to enhance the realism of studies. While fMRI provides valuable insights into which brain areas are activated during aesthetic evaluations, EEG studies offer complementary data by measuring oscillatory brain activity, capturing dynamic changes during aesthetic experiences. Furthermore, EEG can be incorporated into VE providing a valuable way to study neuroarchitecture.

VEs and EEG in Neuroarchitecture

VEs offer immersive, controlled settings that allow researchers to manipulate design elements while maintaining consistency across variables. Recent studies in neuroarchitecture have used virtual reality (VR) combined with neuropsychological tools such as EEG to investigate how architectural environments influence aesthetic perception, emotional responses, and brain activity (Banaei, Ahmadi, & Yazdanfar, 2017; Banaei, Hatami, et al., 2017; Jung et al., 2023; Kober et al., 2012; Mostafavi et al., 2023; Shemesh et al., 2017, 2021, 2022; Slobounov et al., 2015; Taherysayah et al., 2024; Vecchiato, Jelic, et al., 2015, Vecchiato et al., 2015a). Some of these studies used immersive head-mounted displays (HMDs) (e.g., Banaei, Ahmadi, & Yazdanfar, 2017; Banaei, Hatami, et al., 2017), while others relied on desktop-based VR (e.g., Vecchiato et al., 2015a). Immersive systems can enhance spatial presence, potentially intensifying both neural and emotional responses. Therefore, the level of immersion may help explain the variations in findings across different studies. Consequently, differences in technological setups could reveal distinct yet complementary patterns in perception and brain dynamics.

EEG Oscillations and Environment

There are several frequency bands of EEG that have been utilized in previous neuroarchitecture research. This includes alpha, beta, and theta oscillations. Alpha oscillations, which range from 8 to 12 Hz, are frequently associated with attentional regulation and perceptual filtering. In particular, alpha power is thought to reflect the dynamic balance between cortical engagement and inhibition, where alpha desynchronization often indicates active information processing, and synchronization reflects the suppression of irrelevant input (Foxe & Snyder, 2011; Jensen & Mazaheri, 2010; Klimesch, 1999). Rather than simply being linked to a passive state of calm, alpha activity has been shown to modulate based on task demands, including those involving visuospatial attention and environmental perception. For instance, Klimesch (2012) and N. R. Cooper et al. (2003) suggest that alpha synchronization in posterior regions may help suppress distracting stimuli, thereby facilitating focused attention on spatial features. In the context of architectural experience, this suggests that changes in alpha power—particularly in occipital and parietal areas—may reflect how participants selectively attend to complex visual environments such as curved or unfamiliar spatial forms. The present study builds on this view by examining how alpha oscillations vary across aesthetic judgments, with posterior alpha desynchronization indicating heightened perceptual engagement with visually novel architectural boundaries.

On the other hand, higher-order cognitive functions including active thinking, problem solving, and decision making are associated with beta oscillations. Their frequency range is usually between 12 and 30 Hz. Beta activity is linked to environmental perception when processing visual and proprioceptive information needed for

anticipating and interacting with physical obstacles or environmental changes (Di Dona & Ronconi, 2023). It is responsible for segregation or integration and the reorganization of visual inputs. These tasks play a major role in understanding scenes' spatial layout and dynamics. Beta oscillations have also been conceptualized as reflecting the maintenance of the "status quo" in neural systems, supporting ongoing sensorimotor and cognitive states (Engel & Fries, 2010). Moreover, they are thought to facilitate long-range communication across cortical areas, thereby contributing to perceptual integration and top-down control mechanisms (Donner & Siegel, 2011). Prior studies have shown that higher beta power correlates with better performance in visual crowding tasks, which require participants to distinguish a target from surrounding distractors. These findings demonstrate that beta oscillations resolve visual clutter and enhance perceptual clarity. New studies involving transcranial magnetic stimulation provide causal evidence for beta oscillations involved in scene perception and visuospatial processing (Di Dona & Ronconi, 2023; Klimesch, 1999).

Theta oscillations, spanning frequency bands lower than 8 Hz and higher than 4 Hz, are associated with memory load. Theta oscillations have been shown to increase with the complexity of memory load. Regarding scene perception, theta oscillations are crucial for scene-related information in short-term memory (Busch & Herrmann, 2003). Theta oscillations are predominant for binding items to their context during encoding, helping effectively perceive and recall complex scenes (Summerfield & Mangels, 2005).

Aesthetic Judgments on Neural Oscillations

Impacting cognitive assessments, well-being, affection, and behavior patterns, aesthetic experience in architecture is a pronounced mechanism in architectural design and human experience (Adams, 2013; R. Cooper et al., 2014; Gifford, 2002; Hartig, 2008). It is an informative variable that bridges between the built environments and human behavior. To refine how aesthetic experience may affect human behavior, researchers have focused on how sensory, emotional, and cognitive elements shape this experience (Chatterjee & Vartanian, 2014, 2016; Coburn et al., 2017, 2020; Elver Boz et al., 2024a, 2024b).

Chatterjee (2013) explored the relationship between aesthetics and art, characterizing the aesthetic experience as a triad that includes sensations, emotions, and meaning. Chatterjee and Vartanian's (2014) description of the cognitive, emotional, and behavioral components offers a more comprehensive aesthetic perspective. Coburn et al. (2017) outlined how the aesthetic triad designed for aesthetic experiences can be utilized in the neuroscience of architecture, providing a framework for understanding human aesthetic experiences within architectural contexts. Coburn et al. (2020) examined the essential psychological elements of architectural experience (coherence, fascination, and hominess). These dimensions are shaped by the underlying neural systems described in the aesthetic triad model proposed by Chatterjee and Vartanian (2014, 2016). These systems include sensorimotor, emotion valuation, and knowledge-meaning systems, all of which contribute to the aesthetic experience in the built environment. Their study explored the perceived sense of enclosure by assessing whether the environment had open or closed boundaries, along with ceiling height, which varied between high and low, and the boundary shapes of the space, which were either round or square, using fMRI and 2D real environment pictures. The components above are tied to neural activity, influencing aesthetic judgments of various architectural features, for example, enclosure, ceiling height, and curvature. In line with these results, Chatterjee and Vartanian (2014, 2016) observed that aesthetic judgments involve a network of brain areas, particularly the OFC, dorsolateral prefrontal cortex, and anterior insula. Each of these areas plays a crucial role in reward processing, complex cognitive tasks, and emotional awareness, respectively. The simultaneous activation of these areas suggests that the appreciation of architectural features arises from the interaction of emotional, sensory, and cognitive processes.

Further refining this framework, Elver Boz et al. (2024a) introduced familiarity, excitement, and fascination by systematically characterizing the built environment. Their study investigated the perception of curvilinear boundaries and four space properties: size, light, texture, and color that influenced these aesthetic dimensions. Familiarity pointed to the sense of safety, relaxation in an environment, and coherence. Excitement emphasized heightened emotional arousal, while fascination captured environmental complexity and interest with a behavioral propensity to explore. Familiarity, excitement, and fascination—shaping individual experiences in built environments—underscored the importance of aesthetic experiences for designers and neuroscientists. However, neuroarchitecture research has not touched on how key aesthetic judgments on familiarity, excitement, and fascination affect neural oscillations.

The Present Study

Drawing on frameworks established by Coburn et al. (2020) and Elver Boz et al. (2024a), this study explores the neural correlates of aesthetic judgment components for environments with curvilinear boundaries, that is, familiarity, excitement, and fascination, by integrating VR and EEG. The three aesthetic components identified in the studies by Elver Boz et al. (2024a) form an extensive, empirically driven model that describes three fundamental aspects for evaluating the built environment. This study investigates the neural correlations of these aesthetic component concepts. The findings will help bridge the gap between architectural design and neuroscience, providing practical insights for creating environments that promote well-being, comfort, and engagement. The related research questions (RQs) are posed:

RQ1: Are alpha, beta, and theta oscillations influenced by the specific aesthetic judgment (familiarity, excitement, and fascination) during the perception of architectural variables (horizontal vs. vertical boundaries)?

RQ2: Are alpha, beta, and theta oscillations sensitive to architectural variables?

Based on previous research on aesthetic processing and neural oscillations (e.g., Chatterjee & Vartanian, 2014; Elver Boz et al., 2024a; Klimesch, 2011), the following hypotheses are proposed:

Hypothesis 1: Alpha, beta, and theta oscillations will exhibit distinct patterns depending on the specific aesthetic judgment (familiarity, excitement, or fascination), reflecting differential modulation of neural activity.

Hypothesis 2: Oscillatory brain responses will vary depending on architectural variables, with observed differences between horizontal and vertical boundaries, indicating sensitivity to the spatial characteristics of the built environment.

Method

Participants

The experiment involved 20 graduate and undergraduate students from the various departments of I.D Bilkent University, 10 of whom were female and 10 of whom were male. The gender balance in the study was intentionally maintained to reduce variability in oscillatory responses, as previous EEG research has shown that neural activity patterns can differ by sex (Lindsen & Bhattacharya, 2010). The sample size ($N = 20$) aligns with many EEG studies that utilize within-subject designs, particularly in the areas of aesthetic processing and immersive VEs (Hanslmayr et al., 2009; Vecchiato et al., 2015b). Although we did not conduct a prior G-power analysis to determine the sample size—given that this is the first EEG study integrating three aesthetic judgements with different boundary types—we performed a post hoc power analysis to estimate the study's power (Faul et al., 2007).

We used G*Power to conduct a repeated-measures analysis of variance (ANOVA) with 18 within-subject measurements. The factors included two levels of boundary (horizontal and vertical), three levels of electrode location (anterior, central and posterior), three levels of hemisphere (left, right and midline). We observed a partial eta squared of .15 for the three-way interaction effect in the theta band. This value represents the smallest significant effect for conservative post hoc analysis and corresponds to an effect size (f) of .42. With an α level set at .05 and an assumed average correlation among repeated measures of .50, the post hoc analysis showed an achieved power of .97. This confirms that the study was adequately powered to detect the observed within-subject effects.

To equilibrate the participants' neurocognitive development, participants had to be at least 20 years old, with ages 45 and above not being accepted (Brooks et al., 2011; Rosander & Von Hofsten, 2011; Shemesh et al., 2022). A questionnaire was given to those who met the age requirements so that the studies could ascertain whether or not each participant met the inclusion/exclusion requirements. The subjects had normal or corrected to normal vision, no history of neurological disorders, no history of attention deficit hyperactivity disorder, no heart disease, pregnancy, vertigo, or claustrophobia. The Ethics Committee of I.D Bilkent University approved (No: 2023_10_02_01), and the informed consent form was obtained from the subjects. Ishihara's electronic color blindness test measured participants' color accuracy (Color-blindness.com, 2023).

Environmental Stimuli

This study used a set of 32 interior space visualizations, that were systematically designed to manipulate key architectural variables in VE. Each visualization combined four architectural variables, each with two intensity levels: size (small–large), light (dim–bright), texture (lateral–longitudinal), and color (cool–warm). These were categorized into two types of spatial boundaries defined by geometric curvature: horizontal boundaries (HB), which refer to the concave connections of walls and vertical boundaries (VB), which refer to the concave connections of the floor and ceiling (see Figure 1).

Figure 1

Curvilinear Horizontal Boundaries and Curvilinear Vertical Boundaries

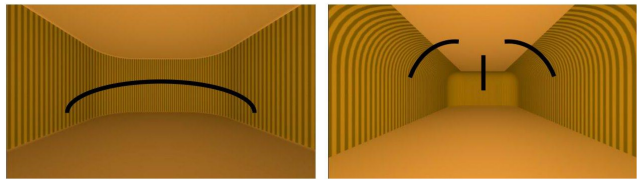

Note. Adapted from "The Aesthetic Experience of Interior Spaces With Curvilinear Boundaries and Various Space Properties in Immersive and Desktop-Based Virtual Environments," by T. Elver Boz, H. Demirkan, and B. A. Urgen, 2024b, *Psychology of Aesthetics, Creativity, and the Arts*. Advance online publication (https://doi.org/10.1037/aca0000723). Copyright 2024 by the American Psychological Association. Adapted with permission. See the online article for the color version of this figure.

According to the spatial definitions established by Elver Boz et al. (2024b), the HB shows the surrounding walls and their geometrical continuity, focusing on the curvilinear connections of the horizontal enclosure. In contrast, the VB refers to the lower and upper surfaces of the interior space—namely the floor and ceiling—and describes the spatial relationship between these surfaces through concave connections.

These visualizations were originally developed and analyzed by Elver Boz et al. (2024b) and have been adapted here as 360-degree video simulations for use in a mobile EEG and VR setup. The participants perceived these zones at eye level. Since the EEG device was used in the study, the visualizations were shown as 360-degree video simulations in the VE to minimize the movement artifacts. The study included 16 HB conditions and 16 VB conditions, resulting in a total of 32 interior video visualizations (see Figure 2).

Instruments and Procedures

The current study employed an integrated experimental design combining immersive VR and EEG to investigate aesthetic judgments in response to architectural environments. Interior spaces were designed digitally using Autodesk 3ds Max, with variations in boundary features to manipulate spatial perception. These environments were rendered as 360-degree panoramic scenes and presented through an HMD, enabling participants to explore each space in an immersive manner. During the task, participants provided aesthetic evaluations across three key dimensions—familiarity, excitement, and fascination—while their neural activity was recorded in real time. This setup allowed for the simultaneous collection of both behavioral and neural data, supporting a comprehensive analysis of the perceptual and affective mechanisms involved in the architectural experience. Figure 3 presents the experiment setup scheme.

The experiment room (I.D Bilkent University G building psychology lab 1), except for the VR + EEG equipment and data acquisition devices, was vacant, colorless, and devoid of windows. The experimental setting would be similar to the one seen in Figure 4.

A participant in the experiment wears a VR headset (C), and there is a controller (E) to respond to appropriate aesthetic judgments; the researcher uses a computer (A), screen (B), and controller (E) within the room to run the experiment, along with high tech computer (HTC) sensors (D) mounted above the ceiling tracking headsets

Figure 2

Virtual Environment Visualizations With Various Space Variables

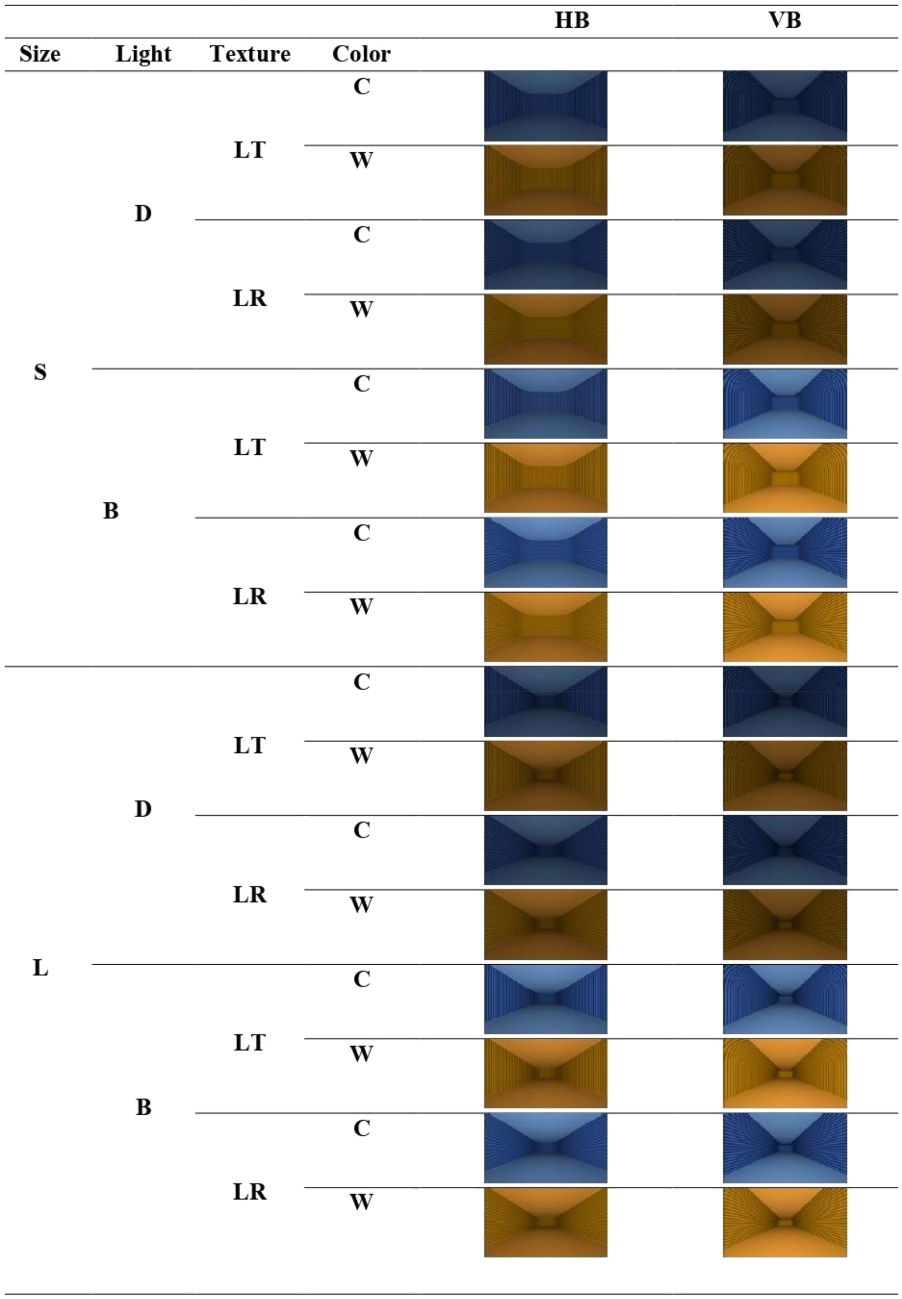

Note. Size as S = small and L = large. Light as B = bright and D = dim. Texture as LT = longitudinal and LR = lateral. Color as C = cool and W = warm. See the online article for the color version of this figure.

(F). The subject has an EEG device placed atop their head and VR equipment for both sessions. In the right corner, the computer runs the experiment, in which the EEG, the VR, and the programs operate concurrently. To make the real-time data easier to follow, the computer simultaneously records it on two screens and gathers it.

The total time for the task section is 60–70 min, including electrode placement and VR glasses adaptation on participants' heads, stimulus presentation, and data acquisition. Participants were asked to move as little as possible throughout the process to minimize EEG noise disruptions.

Figure 3
Experiments Setup Scheme

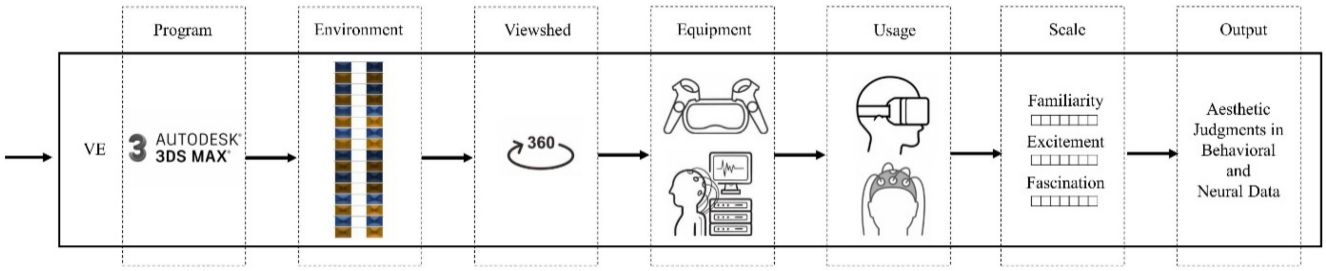

Note. VE = virtual environment. See the online article for the color version of this figure.

The experiment continued in a VR environment generated by Unity's real-time engine and C# scripts experienced by HTC Vive Pro. The study's primary challenge was integrating the HTC Vive VR and the Emotiv EEG recorder (Figure 5). The goal was to capture participant behavioral responses—specifically, aesthetic judgement and neural responses, which refer to brain activity—while presenting a 3D 360-degree visualization of a designed space with different architectural variables, using Unity Engine and C# scripts. Opening ports to incorporate the data sent by C# scripts to the EEG recorder helped to preserve the link between the Emotiv EEG recorder and VR. Start markers for buffers, space visualizations, and reaction tabs were supplied to the ports linked to the emotive EEG recorder during the stimuli display. A general marker ID was assigned to buffers and response tabs. In contrast, a unique marker was assigned to each visualization to indicate the start and for analytical purposes.

To understand the effect of architectural variables of the environment on the aesthetic judgment of participants, mixed-method (quantitative and qualitative) data are required to relate neuroscientific measurements with aesthetic judgment. Emotive (see Figure 6 for EPOC Flex 32-channel mobile brain wear) channels (see Figure 7) obtain physiological data from individuals as they encounter various VE by using HTC Vive Pro. Channels are Fz, F3, F4, F7, F8, FC1, FC2, FC5, FC6, FT9, FT10, Cz, C3, C4, T7, T8, CP1, CP2, CP5, CP6, Pz, P3, P4, P7, P8, PO3, PO4, Oz, O1, O2, O9, and O10. The sensor wires are color-coded. Blue is utilized on the left side (odd numbers), red on the right side (even numbers), and black for reference points. However, for the electrode coding, "F" represents

Figure 4
Example of Experiment Settings

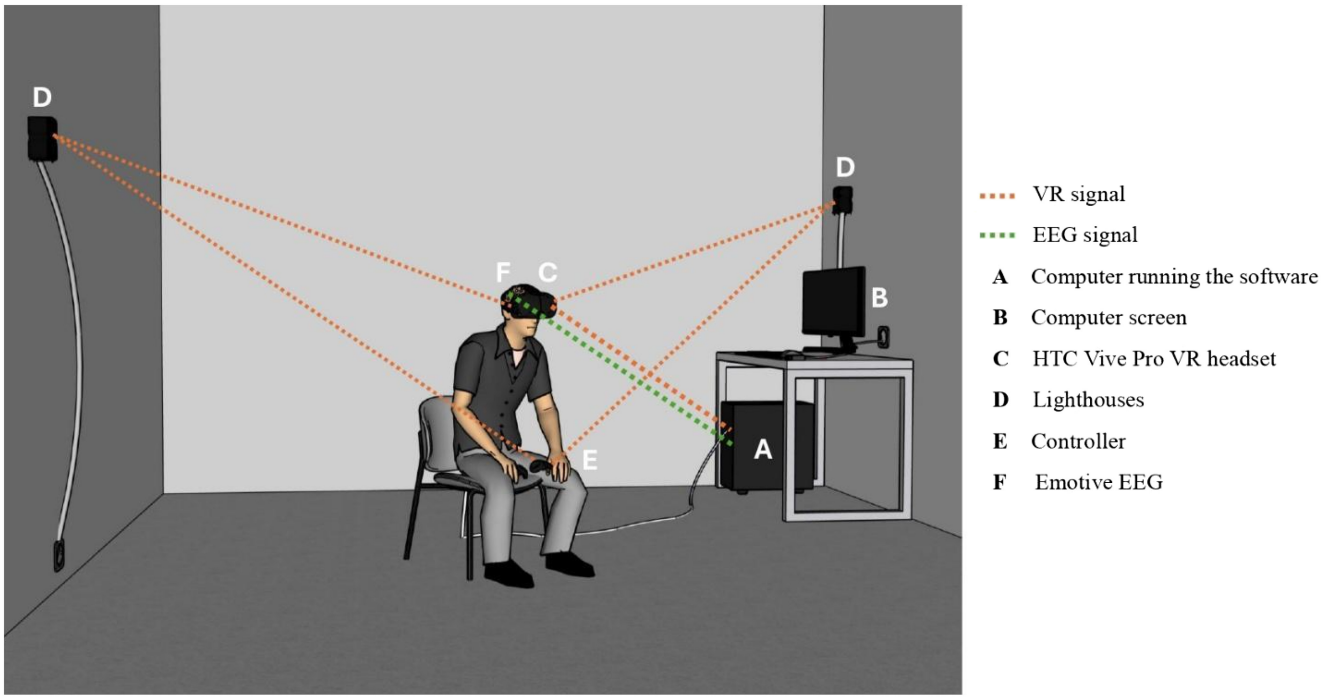

Note. VR = virtual reality; EEG = electroencephalography; HTC = high tech computer. See the online article for the color version of this figure.

Figure 5
Interplay Between EEG and IVE via Ports

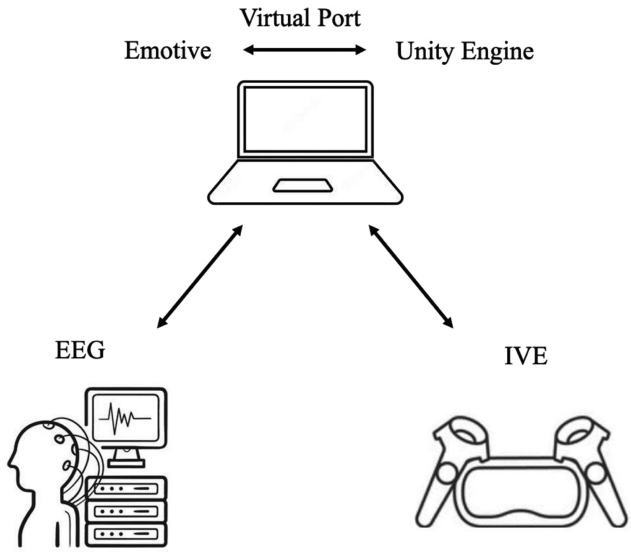

Note. EEG = electroencephalography; IVE = immersive virtual environment.

frontal channels, "C" defines central channels, "T" presents temporal channels, "P" symbolizes parietal channels, and "O" depicts occipital channels.

Before the experiment began, the study identified a physical interference between the EEG cap and the VR headset, which made it impossible to use four electrode sites in their standard positions.

Figure 6
Participants Were Wearing the EEG Headset and the VR HTC Vive Pro

Note. EEG = electroencephalography; VR = virtual reality; HTC = high tech computer. See the online article for the color version of this figure.

These sites were Fp1 and Fp2 on the forehead, and TP9 and TP10 on the sides of the head. To maintain a 32-channel setup, these electrodes were relocated to alternative positions: Fp1 and Fp2 were repositioned to O9 and O10 (occipital), and TP9 and TP10 to PO3 and PO4 (parieto-occipital). This adjustment followed the international 10–20 system and aligned with the Emotiv EPOC Flex electrode configuration. By making this modification, it was ensured that the headset could be worn comfortably while maintaining EEG data quality and spatial accuracy.

Participants were shown 32 randomized videos throughout the session as part of the study procedure. One video was shown at a time during the task, with a question answered following each presentation. The session was separated into three blocks, and according to the three aesthetic components, the stimuli would be assessed: familiarity, excitement, and fascination.

Each participant's blocks were assigned at random. The sequence of blocks was randomized for each participant, ensuring that every individual experienced the aesthetic judgment tasks in a unique order. Additionally, the order of video presentations within each block was also randomized, meaning that participants viewed a different randomized sequence of the 32 videos for each of the three aesthetic component conditions. For each video, participants rated their experience using a 7-point Likert scale. Participants used VR controllers to make their evaluations. All participants experienced the environment within the same time frame and followed the same 360-degree visual sequence, meaning that free navigation within the space was not allowed. At the end of each block, participants were asked to confirm whether they were willingness to continue with the experiment.

Each trial began with a 5-s buffer screen displaying a fixation cross, followed by the video presentation. The video stimuli were presented for 10 s, a duration adopted from a previous study using the same VE visualizations (Elver Boz et al., 2024b), where 10 s was found to be sufficient for aesthetic evaluation without causing fatigue or disengagement. Following the video, participants were asked to rate the space in the video depending on the question posed. Participants had a 5-s window to select one of the interactive buttons, with responses thoroughly logged. Missed responses were recorded when there was no response within 5 s. Notably, at the start of each trial, EEG triggers were sent to the Emotive EEG recorder at the start of the buffer, the start of the video, and the start of the question, allowing for synchronous integration of neurophysiological data. Figure 8 demonstrates the trial flow within each block.

Data Analysis

In the behavioral data (participants' responses), based on the ratings of the 20 participants, the paired-sample *t* test was conducted on behavioral data to compare participants' aesthetic ratings across boundary types (horizontal vs. vertical) within each judgment dimension: familiarity, excitement, and fascination. In the neural data, the same 20 participants' records were collected. Following preprocessing with EEGLAB (Delorme & Makeig, 2004), manual artifact rejection procedures were applied to the EEG data. EEG recordings of each participant were examined. EEG data were bandpass-filtered between 0.5 and 40 Hz to reduce slow drifts and high-frequency noise (such as muscular movements), as recommended in standard EEG preprocessing protocols (Cohen, 2014;

Figure 7

Emotiv 32-Channel Epoc Flex EEG Headset Electrode Distribution Map and Segmentation of 10 Brain Areas

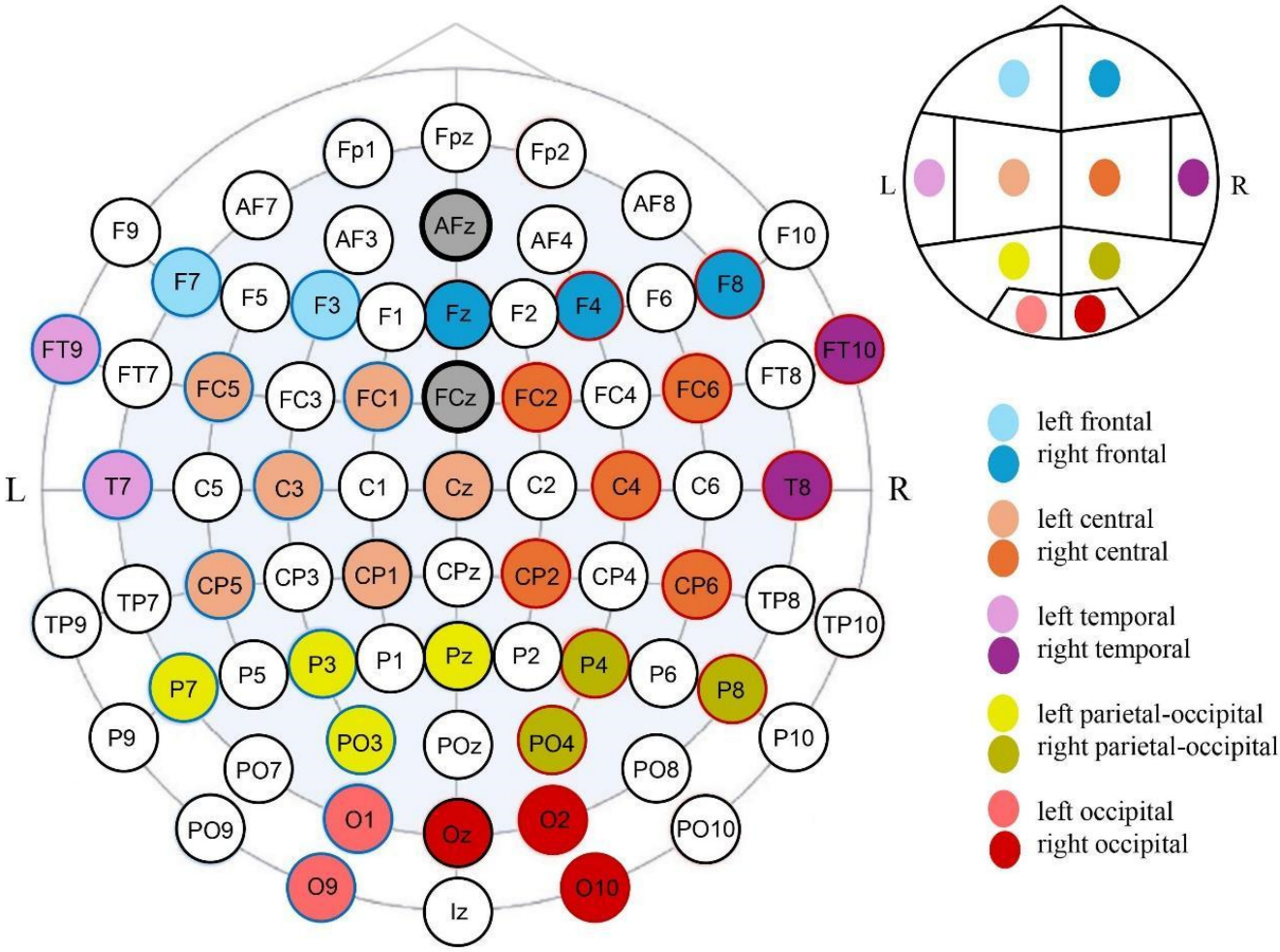

Note. EEG = electroencephalography. See the online article for the color version of this figure.

Luck, 2014), while retaining the frequency range associated with cognitive operations. No channels were eliminated; instead, each was preprocessed to observe individual outputs without elimination. In cases where channels exhibited excessive noise or deviated substantially from expected signal patterns, interpolation was applied to correct for poor-quality recordings and ensure consistency in the data set (Keil et al., 2014). To standardize the EEG signals across channels, an average reference projection was applied. Specifically, the EEG data were rereferenced using an average reference montage (Nunez & Srinivasan, 2006). This method helps reduce variability dependent on the reference while preserving the original signal dynamics through projection, rather than permanent subtraction. Subsequently, muscle artifacts were visually inspected and manually removed by identifying segments with excessive high-frequency activity (typically above 30 Hz) that were not attributable to cognitive processes. These segments were manually excluded from further analysis, following standard artifact rejection practices in EEG research (Keil et al., 2014; Luck, 2014). Independent component analysis (ICA) was employed to capture ocular artifacts, such as eye blinks and saccades. The ICA decomposition was performed using the runica algorithm (Makeig et al., 1996) with 20 components. Eye-related artifacts were automatically detected through correlation with electrooculogram channels. These components were then visually inspected and manually excluded from the data, ensuring that only nonartifactual neural signals were retained for further analysis.

The time-frequency decomposition of EEG signals was performed using event-related spectral perturbation (ERSP) analysis in EEGLAB (Delorme & Makeig, 2004). ERSPs provide a dynamic representation of changes in spectral power relative to baseline activity, making them particularly effective for analyzing oscillatory responses to temporally locked events in aesthetic judgment tasks. Each stimulus lasted for 10 s, but we limited our ERSP analysis to a 2-s window following the stimulus. Previous research has shown that ERSPs are most pronounced shortly after a stimulus, reflecting immediate cognitive and perceptual processing (Pfurtscheller & Lopes da Silva, 1999). Using an extended window could dilute the effect of temporally specific oscillatory responses. Therefore, a 2-s window allows for a focused analysis of the time-locked

Figure 8

Time Sequence Programmed for EEG, Repeating 32 Times in Each Trial

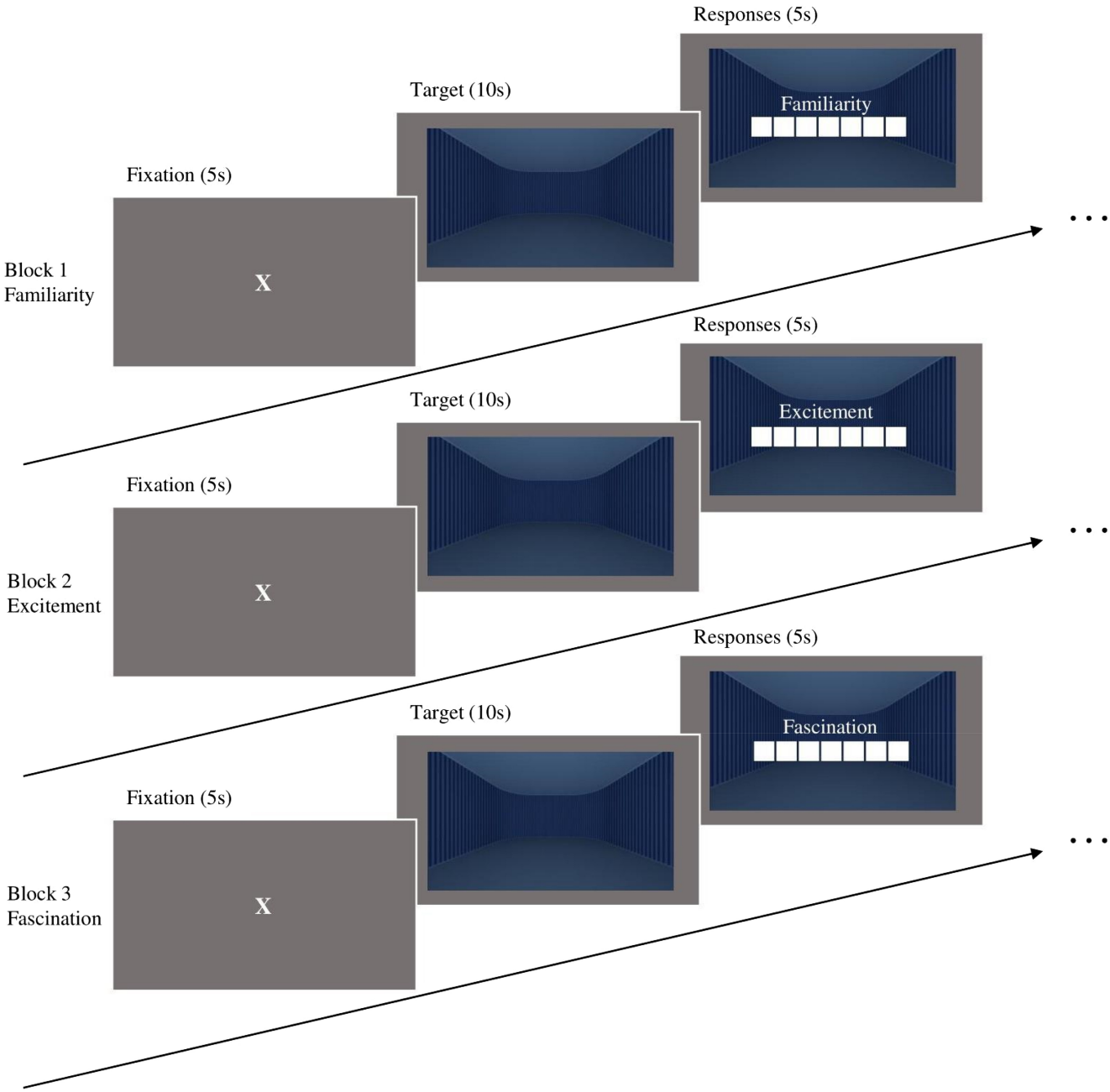

Note. EEG = electroencephalography. See the online article for the color version of this figure.

spectral dynamics that are relevant to aesthetic judgments. For each participant, ERSPs were computed for the theta (4–7 Hz), alpha (8–13 Hz), and beta (13–30 Hz) frequency bands across 1,000 ms epochs that were time-locked to stimulus onset.

To analyze oscillatory brain activity associated with aesthetic judgments, the study used EEGLAB's group-level ERSP computation pipeline. Time–frequency decompositions were performed using Morlet wavelets over a frequency range of 0–30 Hz. A baseline correction was applied using the prestimulus interval from −1,000 to 0 ms, ensuring that ERSP values accurately reflected stimulus-related changes in power. ERSPs were precomputed across all channels (using std_precom function) and averaged within nine predefined scalp areas of interest (region of interests), representing anterior, central, and posterior areas across both hemispheres. For each participant and condition, mean ERSP values were extracted for the theta (4–7 Hz), alpha (8–12 Hz), and beta (13–30 Hz) bands. Repeated-measures ANOVAs were conducted with a 2 (boundary type: HB, VB) × 3 (electrode location: anterior, central, posterior) × 3 (hemisphere: left,

midline, right) design. Electrode clusters were grouped as follows: anterior, Fz/F3/F4/F7/F8/FC1/FC2/FC5/FC6/FT9/FT10; central, Cz/C3/C4/T7/T8/CP1/CP2/CP5/CP6; and posterior, Pz/P3/P4/P7/P8/PO3/PO4/Oz/O1/O2/O9/O19 areas.

Results

Aesthetic Judgment Dimensions and Architectural Variables in Behavioral Data

The study examined spaces with different architectural variables in three primary aesthetic judgment dimensions. In the familiarity component, the HB was more familiar than the VB, $t(19) = 4.75$, $p < .001$, $d = 1.06$. The mean number of HB on familiarity ($M = 4.99$, $SD = 1.18$) and VB on familiarity ($M = 2.74$, $SD = 1.05$) differ significantly. The average difference between the paired mean score values familiarity HB and familiarity VB mean values is 2.25.

In the excitement component, the VB was given higher scores than the HB, $t(19) = 4.19$, $p < .001$, $d = 0.94$. The mean values of VB on excitement ($M = 4.53$, $SD = 1.14$) and HB on excitement ($M = 3.15$, $SD = 1.03$) differ significantly. The average difference between the paired mean score values excitement VB and excitement HB mean values is 1.38.

In the fascination components, the VB was given higher scores than the HB, $t(19) = 7.87$, $p < .001$, $d = 1.76$. The mean number of VB in fascination VB ($M = 5.17$, $SD = 0.91$) and HB on fascination ($M = 2.87$, $SD = 0.65$) differ significantly. The average difference between the paired mean score values familiarity VB and familiarity HB mean values is 2.30. The aesthetic judgment dimensions and architectural variables in behavioral data are shown in Figure 9.

Figure 9

Violin Plot of Aesthetic Judgment Dimensions—Familiarity, Excitement, and Fascination—Across Two Architectural Boundary Conditions: HB and VB

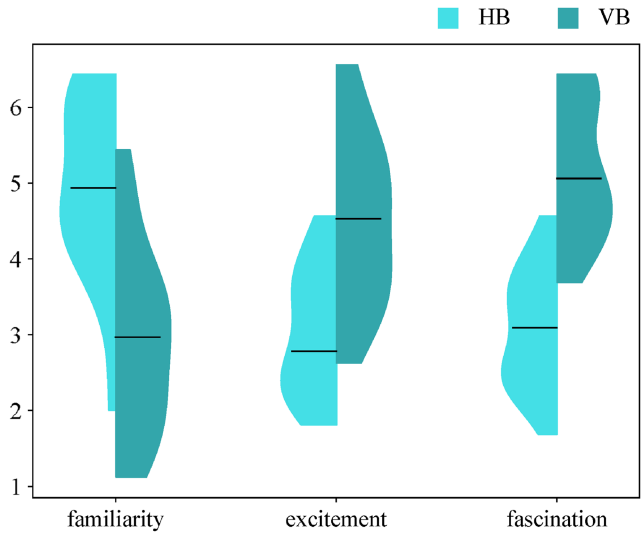

Note. The black horizontal lines represent the mean scores for each condition. The shape and width of each violin represent the kernel density estimation of participant responses, reflecting the relative frequency of ratings on a scale from 1 to 7. HB = horizontal boundaries; VB = vertical boundaries. See the online article for the color version of this figure.

Aesthetic Judgment Dimensions and Architectural Variables in Neural Data

To investigate how oscillatory activity related to each aesthetic judgement varied based on boundary type, areas (electrode locations), and hemispheres, we ran repeated-measures ANOVAs separately for the theta, alpha, and beta frequency bands. These analyses were performed for each dimension of aesthetic judgment—familiarity, excitement, and fascination. We applied Mauchly's test of sphericity to assess the sphericity assumption, applying Greenhouse–Geisser corrections where violations were detected.

Oscillatory Activity in Familiarity Judgments

Alpha Band in Familiarity Judgments. The analysis revealed a significant main effect of boundary type, $F(1, 19) = 10.33$, $p = .005$, $\eta_p^2 = .35$, indicating that alpha power significantly differed between HB and VB. Bonferroni-corrected post hoc comparisons showed that desynchronization was significantly greater under VB compared to HB, $t(19) = 3.21$, $p = .005$, $d = 0.38$.

There was also a significant main effect of electrode location, $F(1.14, 21.66) = 15.61$, $p < .001$, $\eta_p^2 = .45$, reflecting differences across anterior, central, and posterior sites. Additionally, follow-up comparisons indicated that posterior sites showed significantly greater desynchronization compared to anterior, $t(19) = 4.35$, $p = .001$, $d = 0.83$, and central sites, $t(19) = 3.84$, $p = .003$, $d = 0.86$.

The main effect of hemisphere was also significant, $F(1.42, 26.94) = 4.12$, $p = .040$, $\eta_p^2 = .18$. However, Bonferroni-corrected post hoc comparisons between the left, midline, and right hemispheres did not reveal any statistically significant pairwise differences (all $p > .10$). This indicates that while the hemisphere factor had a significant overall effect, none of the specific pairwise comparisons remained significant after correction.

A significant Boundary Type × Electrode Location interaction was observed, $F(1.53, 29.05) = 8.76$, $p = .002$, $\eta_p^2 = .32$, indicating that the effect of boundary type varied across cortical area. Post hoc comparisons showed that the posterior VB elicited greater desynchronization compared to several other conditions. Specifically, it showed significant differences when compared to the following: the anterior HB, $t(19) = 5.24$, $p < .001$, $d = 1.27$, the center HB, $t(19) = 5.43$, $p < .001$, $d = 1.34$, the posterior HB, $t(19) = 3.46$, $p = .040$, $d = 0.70$, the anterior VB, $t(19) = 5.70$, $p < .001$, $d = 1.09$, and the center VB, $t(19) = 4.46$, $p = .004$, $d = 1.07$.

A significant Boundary Type × Hemisphere interaction also emerged, $F(2, 38) = 13.06$, $p < .001$, $\eta_p^2 = .41$, suggesting lateralized effects of boundary conditions on alpha power. VB induced greater desynchronization compared to HB across the left hemisphere, $t(19) = 3.40$, $p = .045$, $d = 0.52$, the right hemisphere, $t(19) = 3.89$, $p = .015$, $d = 0.53$, and the midline, $t(19) = 3.55$, $p = .032$, $d = 0.56$. Additionally, midline VB was significantly lower than left VB, $t(19) = -3.80$, $p = .018$, $d = -0.39$, and right VB showed greater strength than midline VB, $t(19) = 3.82$, $p = .017$, $d = 0.39$. These findings suggest a dominance in the posterior-right area.

The Electrode Location × Hemisphere interaction was also significant, $F(2.82, 53.65) = 5.60$, $p = .002$, $\eta_p^2 = .23$, indicating that alpha activity varied with scalp lateralization. Specifically, the posterior midline exhibited significantly greater desynchronization compared to the anterior left, $t(19) = 4.83$, $p = .004$, $d = 0.42$. Additionally, the posterior right showed stronger suppression than both the anterior

left, $t(19) = 4.42$, $p = .011$, $d = 1.06$, and the center left, $t(19) = 4.02$, $p = .027$, $d = 1.10$. Furthermore, the posterior left was significantly greater than the anterior right, $t(19) = -4.24$, $p = .016$, $d = -0.94$, and the posterior right was higher than the center midline, $t(19) = 3.92$, $p = .033$, $d = 1.19$. The posterior midline also surpassed the anterior right, $t(19) = -5.61$, $p < .001$, $d = -0.49$, while the posterior right showed stronger suppression than the anterior right, $t(19) = 4.71$, $p = .006$, $d = 1.12$, and the center right, $t(19) = 4.43$, $p = .010$, $d = 1.11$.

Finally, the three-way Boundary Type × Electrode Location × Hemisphere interaction was significant, $F(4, 76) = 3.21$, $p = .017$, $\eta_p^2 = .14$, indicating that the combined effects of spatial configuration and hemispheric asymmetry varied across topographic sites. Post hoc comparisons showed that the strongest alpha desynchronization occurred in the posterior VB area. For example, the anterior left HB showed significantly lower suppression compared to the posterior left VB, $t(19) = 5.03$, $p = .011$, $d = 1.41$, the posterior midline VB, $t(19) = 5.14$, $p = .009$, $d = 0.80$, and the posterior right VB, $t(19) = 5.87$, $p = .002$, $d = 1.76$. Similarly, the center left HB had lower desynchronization than the posterior right HB, $t(19) = 5.07$, $p = .017$, $d = 1.50$, the posterior midline VB, $t(19) = 4.99$, $p = .012$, $d = 0.87$, and the posterior right VB, $t(19) = 5.70$, $p = .003$, $d = 1.84$. The center right HB was also reduced in comparison to the posterior left VB, $t(19) = 4.97$, $p = .013$, $d = 1.38$, the posterior midline VB, $t(19) = 4.68$, $p = .025$, $d = 0.77$, and the posterior right VB, $t(19) = 5.91$, $p = .002$, $d = 1.72$. Among VB sites, the anterior left showed lower desynchronization than the posterior left, $t(19) = 4.61$, $p = .029$, $d = 1.03$, the posterior midline, $t(19) = 4.47$, $p = .040$, $d = 0.42$, and the posterior right, $t(19) = 5.34$, $p = .006$, $d = 1.37$. The posterior left VB was significantly greater than the anterior midline, $t(19) = -4.44$, $p = .043$, $d = -1.31$, and the anterior right VB, $t(19) = -5.56$, $p = .004$, $d = -1.20$. Additionally, the anterior midline VB was lower than the posterior midline, $t(19) = 4.52$, $p = .036$, $d = 0.70$, and the posterior right VB, $t(19) = 5.24$, $p = .007$, $d = 1.65$. The center midline VB was also lower than the posterior right VB, $t(19) = 4.94$, $p = .014$, $d = 1.63$. Furthermore, the posterior midline VB was lower than the posterior right VB, $t(19) = 4.65$, $p = .027$, $d = 0.95$. Both the anterior right and center right VB were significantly lower than the posterior right VB, with results showing, $t(19) = 5.60$, $p = .003$, $d = 1.54$ and $t(19) = 5.17$, $p = .008$, $d = 1.52$, respectively.

Beta Band in Familiarity Judgments. The analysis revealed several significant effects. Firstly, there was a main effect of boundary type, $F(1, 19) = 12.63$, $p = .002$, $\eta_p^2 = .40$, indicating greater activity for VB compared to HB. However, post hoc comparisons showed significantly higher beta power under HB compared to VB, $t(19) = 3.55$, $p = .002$, $d = 0.50$.

There was a robust main effect of electrode location, $F(1.10, 20.83) = 30.77$, $p < .001$, $\eta_p^2 = .62$, demonstrating significant variation in beta activity across anterior, central, and posterior area. Post hoc analyses revealed that the center sites exhibited significantly greater beta power compared to the anterior sites, $t(19) = 4.27$, $p = .001$, $d = 0.33$. Additionally, the posterior sites showed higher beta power than both the anterior sites, $t(19) = 5.65$, $p < .001$, $d = 1.21$, and the center sites, $t(19) = 5.63$, $p < .001$, $d = 0.88$.

The main effect of hemisphere was also significant, $F(1.51, 28.59) = 4.88$, $p = .023$, $\eta_p^2 = .20$, indicating differences across left, midline, and right hemispheres. Bonferroni-corrected post hoc comparisons showed that beta power was significantly greater at the midline compared to the right hemisphere, $t(19) = 2.87$, $p = .029$, $d = 0.29$.

A significant Boundary Type × Electrode Location interaction was observed, $F(2, 38) = 3.80$, $p = .031$, $\eta_p^2 = .17$, suggesting regional variation in boundary effects. Specifically, beta power in the anterior HB condition was found to be significantly greater than in several other conditions: anterior VB, $t(19) = 4.44$, $p = .004$, $d = 0.59$, center VB, $t(19) = 4.79$, $p = .002$, $d = 0.70$, posterior VB, $t(19) = 5.69$, $p < .001$, $d = 1.88$, and posterior HB, $t(19) = 4.23$, $p = .007$, $d = 1.12$. Additionally, the center HB exhibited higher beta power compared to posterior HB, $t(19) = 3.55$, $p = .032$, $d = 0.58$, and posterior VB, $t(19) = 4.80$, $p = .002$, $d = 1.34$. Moreover, center VB showed greater beta power than posterior VB, $t(19) = 5.55$, $p < .001$, $d = 1.18$. Within the VB conditions, beta power in the posterior area was greater than in the anterior area, $t(19) = 5.45$, $p < .001$, $d = 1.29$.

The interaction between boundary type and hemisphere was also significant, $F(2, 38) = 13.40$, $p < .001$, $\eta_p^2 = .41$, indicating that the effect of boundary condition on beta power was lateralized. Post hoc analyses revealed that beta power was significantly greater at the left HB compared to both the left VB, $t(19) = 3.88$, $p = .015$, $d = 0.76$, and the right VB, $t(19) = 4.36$, $p = .005$, $d = 0.79$. Under VB, beta power at the midline was significantly greater than at both the left, $t(19) = -4.08$, $p = .010$, $d = 0.53$, and right hemispheres, $t(19) = 4.11$, $p = .009$, $d = 0.55$. Additionally, beta power was significantly higher at right HB compared to the right VB, $t(19) = 3.76$, $p = .020$, $d = 0.64$.

Furthermore, the Electrode Location × Hemisphere interaction reached significance, $F(2.53, 48.03) = 7.67$, $p = .001$, $\eta_p^2 = .29$, indicating that beta activity varied by hemisphere across scalp area. Post hoc comparisons showed that in the anterior area, the left hemisphere exhibited greater beta power than the posterior left, $t(19) = 4.12$, $p = .021$, $d = 1.02$, posterior midline, $t(19) = 4.21$, $p = .017$, $d = 0.76$, and posterior right, $t(19) = 4.76$, $p = .005$, $d = 1.52$, area. Additionally, beta power in the center-left area was greater than in the posterior left, $t(19) = 4.18$, $p = .018$, $d = 0.72$, posterior midline, $t(19) = 3.85$, $p = .039$, $d = 0.45$, and posterior right, $t(19) = 5.52$, $p < .001$, $d = 1.22$, area, but lower than in the anterior right area, $t(19) = -4.15$, $p = .020$, $d = 0.59$. Moreover, midline anterior sites also exhibited higher beta power compared to the posterior midline, $t(19) = 5.76$, $p < .001$, $d = 0.79$, and posterior right, $t(19) = 5.12$, $p = .002$, $d = 1.55$, area; midline center beta power was observed to be higher than both, $t(19) = 6.81$, $p < .001$, $d = 0.76$; $t(19) = 5.31$, $p = .001$, $d = 1.52$.

Finally, the three-way interaction among boundary type, electrode location, and hemisphere did not reach significance. These findings suggest that beta-band activity during familiarity judgments was modulated by boundary condition across both electrode locations and hemispheres, with particularly strong effects observed in posterior and midline area.

Theta Band in Familiarity Judgments. The analysis revealed a significant main effect of boundary type, $F(1, 19) = 24.26$, $p < .001$, $\eta_p^2 = .56$. Bonferroni-corrected post hoc comparisons confirmed that theta power was significantly higher under VB compared to HB, $t(19) = 4.93$, $p < .001$, $d = 0.75$. However, the main effect of electrode location and hemisphere was not significant.

A significant Boundary Type × Electrode Location interaction was identified, $F(1.48, 28.12) = 4.00$, $p = .040$, $\eta_p^2 = .17$, indicating

topographical differences in theta activity related to boundary types. Post hoc comparisons revealed that theta power was significantly greater in the anterior VB condition compared to the center VB, $t(19) = 8.08$, $p < .001$, $d = 0.86$. Additionally, the posterior VB was significantly greater theta power than the anterior HB, $t(19) = 3.39$, $p = .046$, $d = 1.18$. Furthermore, theta power in the center VB exceeded that of the center HB, $t(19) = 6.28$, $p < .001$, $d = 0.65$. The posterior VB was also showed greater theta power than the center HB, $t(19) = 3.95$, $p = .013$, $d = 1.12$, and the center VB was greater than the posterior HB, $t(19) = 6.18$, $p < .001$, $d = 0.80$.

Additionally, the Boundary Type × Hemisphere interaction was significant, $F(2, 38) = 5.83$, $p = .006$, $\eta_p^2 = .24$, suggesting lateralized modulation of boundary effects. Post hoc comparisons revealed that theta power was significantly greater in the left VB condition compared to the left HB, $t(19) = 4.73$, $p = .002$, $d = 1.09$. Additionally, midline VB showed greater theta power than left HB, $t(19) = 5.64$, $p < .001$, $d = 0.95$, and right VB also was greater than left HB, $t(19) = 3.76$, $p = .020$, $d = 1.04$. Furthermore, left VB exhibited greater theta power than midline HB, $t(19) = 3.67$, $p = .024$, $d = 0.80$, and midline VB was greater than midline HB, $t(19) = 4.77$, $p = .002$, $d = 0.67$. Lastly, midline VB showed greater theta power than right HB, $t(19) = 3.91$, $p = .014$, $d = 0.40$.

An interaction between Electrode Location × Hemisphere was also significant, $F(2.11, 40.15) = 6.29$, $p = .004$, $\eta_p^2 = .25$, indicating that theta power distribution varied by lateralized scalp area. Bonferroni-corrected post hoc comparisons showed that theta power was significantly higher in the center left VB condition compared to the following: center left HB, $t(19) = 6.96$, $p < .001$, $d = 0.78$, posterior left HB, $t(19) = 6.31$, $p < .001$, anterior midline HB, $t(19) = 4.52$, $p = .036$, $d = 0.81$, posterior midline HB, $t(19) = 7.74$, $p < .001$, $d = 0.92$, and anterior right HB, $t(19) = 6.49$, $p < .001$, $d = 0.94$.

In the midline, center midline VB showed significantly higher theta power compared to center left HB, $t(19) = 5.66$, $p = .003$, $d = 0.79$, posterior left HB, $t(19) = 6.29$, $p < .001$, anterior midline HB, $t(19) = 4.58$, $p = .031$, $d = 0.82$, posterior midline HB, $t(19) = 6.46$, $p < .001$, $d = 0.93$, and anterior right HB, $t(19) = 5.43$, $p = .005$, $d = 0.95$.

Additionally, the center right VB condition showed greater theta power than center left HB, $t(19) = 4.77$, $p = .020$, $d = 0.80$, posterior left HB, $t(19) = 5.22$, $p = .008$, anterior midline HB, $t(19) = 4.38$, $p = .049$, $d = 0.84$, posterior midline HB, $t(19) = 5.47$, $p = .004$, $d = 0.95$, and anterior right HB, $t(19) = 4.95$, $p = .013$, $d = 0.96$.

Finally, the three-way interaction among boundary type, electrode location, and hemisphere was significant, $F(2.32, 44.07) = 3.42$, $p = .035$, $\eta_p^2 = .15$, indicating that theta dynamics were jointly influenced by boundary configuration and hemispheric organization across different cortical sites. Bonferroni-corrected post hoc comparisons revealed that theta power was significantly higher in the center left VB compared to the following: anterior left HB, $t(19) = 5.49$, $p = .004$, $d = 0.80$, center midline VB, $t(19) = 4.80$, $p = .019$, $d = 0.80$, and center right VB, $t(19) = 4.76$, $p = .021$, $d = 0.82$. Additionally, center midline VB showed higher theta power than posterior left HB, $t(19) = 6.29$, $p < .001$, anterior right HB, $t(19) = 5.43$, $p = .005$, $d = 0.95$, and center right HB, $t(19) = 4.55$, $p = .034$, $d = 0.62$. The results of repeated-measures ANOVAs conducted on alpha, beta, and theta power for the familiarity judgments are presented in Table 1.

Table 1
Repeated-Measures ANOVA Results for Alpha, Beta, and Theta Band Power in the Familiarity Judgment

Familiarity	Alpha	Beta	Theta
Boundary type	**$F(1, 19) = 10.33, p = .005, \eta_p^2 = .35$**	**$F(1, 19) = 12.63, p = .002, \eta_p^2 = .40$**	**$F(1, 19) = 24.26, p < .001, \eta_p^2 = .56$**
Electrode location	**$F(1.14, 21.66) = 15.61, p < .001, \eta_p^2 = .45$**	**$F(1.10, 20.83) = 30.77, p < .001, \eta_p^2 = .62$**	$F(1.25, 23.72) = 3.55$, $p = .064$
Hemisphere	**$F(1.42, 26.94) = 4.12, p = .040, \eta_p^2 = .18$**	**$F(1.51, 28.59) = 4.88, p = .023, \eta_p^2 = .20$**	$F(2, 38) = 2.21$, $p = .124$
Boundary Type × Electrode Location	**$F(1.53, 29.05) = 8.76, p = .002, \eta_p^2 = .32$**	**$F(2, 38) = 3.80, p = .031, \eta_p^2 = .17$**	**$F(1.48, 28.12) = 4.00, p = .040, \eta_p^2 = .17$**
Boundary Type × Hemisphere	**$F(2, 38) = 13.06, p < .001, \eta_p^2 = .41$**	**$F(2, 38) = 13.40, p < .001, \eta_p^2 = .41$**	**$F(2, 38) = 5.83, p = .006, \eta_p^2 = .24$**
Electrode Location × Hemisphere	**$F(2.82, 53.65) = 5.60, p = .002, \eta_p^2 = .23$**	**$F(2.53, 48.03) = 7.67, p = .001, \eta_p^2 = .29$**	**$F(2.11, 40.15) = 6.29, p = .004, \eta_p^2 = .25$**
Boundary Type × Electrode Location × Hemisphere	**$F(4, 76) = 3.21, p = .017, \eta_p^2 = .14$**	$F(4, 76) = 0.78$, $p = .543$	**$F(2.32, 44.07) = 3.42, p = .035, \eta_p^2 = .15$**

Note. Bold values indicate statistically significant effects ($p < .05$). ANOVA = analysis of variance.

Oscillatory Activity in Excitement Judgments

Alpha Band in Excitement Judgments. The analysis revealed a significant main effect of boundary type, $F(1, 19) = 11.32$, $p = .003$, $\eta_p^2 = .37$, indicating a difference in alpha power based on boundary types. Post hoc analyses confirmed significantly greater alpha desynchronization under VB compared to HB, $t(19) = 3.36$, $p = .003$, $d = 0.60$.

The main effect of electrode location was also significant, $F(1.45, 27.53) = 23.71$, $p < .001$, $\eta_p^2 = .55$, reflecting variations across anterior, central, and posterior area. Post hoc comparisons revealed that posterior sites exhibited significantly greater alpha power than both anterior, $t(19) = 5.69$, $p < .001$, $d = 0.82$, and central sites, $t(19) = 4.75$, $p < .001$, $d = 0.73$.

Additionally, a significant main effect of hemisphere was found, $F(2, 25.38) = 7.04$, $p < .001$, $\eta_p^2 = .27$, suggesting asymmetries in alpha activity between the hemispheres. Post hoc analyses showed that midline electrodes exhibited significantly greater alpha power compared to the right hemisphere, $t(19) = 3.69$, $p = .005$, $d = 0.45$.

The interaction between Boundary Type × Electrode location did not reach significance. However, the interaction between Boundary Type × Hemisphere was significant, $F(1.33, 25.21) = 4.37$, $p = .037$, $\eta_p^2 = .19$. Post hoc analyses revealed that right hemisphere responses under VB elicited significantly greater alpha desynchronization than left HB, $t(19) = 3.38$, $p = .047$, $d = 1.06$, midline HB, $t(19) = 3.41$, $p = .044$, $d = 0.85$, and midline VB, $t(19) = 3.83$, $p = .017$, $d = 0.38$.

Moreover, a significant interaction between Electrode Location × Hemisphere was also observed, $F(1.61, 30.52) = 7.72$, $p = .003$, $\eta_p^2 = .29$. Post hoc comparisons showed that posterior right sites exhibited significantly higher alpha power compared to the following: anterior left, $t(19) = 4.67$, $p = .006$, $d = 1.68$, posterior midline, $t(19) = 3.81$, $p = .042$, $d = 1.36$, anterior midline, $t(19) = 4.79$, $p = .005$, $d = 1.64$, center midline, $t(19) = 4.81$, $p = .004$, $d = 1.56$, anterior right, $t(19) = 4.53$, $p = .008$, $d = 1.63$, and center right, $t(19) = 4.88$, $p = .004$, $d = 1.57$.

Finally, the three-way interaction among boundary type, electrode location, and hemisphere was significant, $F(2.12, 40.34) = 4.70$, $p = .013$, $\eta_p^2 = .20$, indicating that alpha activity was influenced by the combined effects of spatial electrode position, hemispheric lateralization, and boundary configuration. Post hoc comparisons revealed that the posterior left VB showed significantly greater desynchronization compared to the anterior left VB, $t(19) = 4.60$, $p = .030$, $d = 1.81$. Additionally, the posterior right HB showed stronger responses than the center left HB, $t(19) = 4.92$, $p = .015$, $d = 1.87$. Moreover, the posterior right HB was significantly greater than both posterior left VB, $t(19) = 4.42$, $p = .046$, $d = 1.75$, and the anterior right HB, $t(19) = 4.64$, $p = .027$, $d = 1.59$.

The center right HB also exceeded the posterior right HB, $t(19) = 4.91$, $p = .015$, $d = 1.96$, while the posterior left VB was higher than the center right HB, $t(19) = 4.42$, $p = .045$, $d = 1.51$. In contrast, the posterior midline HB was lower than the anterior right HB, $t(19) = -4.57$, $p = .032$, $d = -1.30$, the anterior midline VB, $t(19) = -4.77$, $p = .020$, $d = -1.57$, and the center midline VB, $t(19) = -4.84$, $p = .017$, $d = -1.57$.

Moreover, the anterior left VB was significantly greater than both the posterior left VB, $t(19) = 5.74$, $p = .002$, $d = 0.80$, and the posterior right VB, $t(19) = 4.65$, $p = .027$, $d = 1.00$. Finally, the center left VB was greater than the posterior left VB, $t(19) = 4.69$, $p = .024$, $d = 1.00$, while the posterior left VB was lower than the anterior midline VB, $t(19) = -5.15$, $p = .009$, $d = -1.13$, the center midline VB, $t(19) = -5.20$, $p < .001$, $d = -1.12$, the anterior right VB, $t(19) = -5.23$, $p = .007$, $d = -0.98$, and the center right VB, $t(19) = -4.84$, $p = .018$, $d = -0.94$. Additionally, both the anterior midline VB, $t(19) = 4.48$, $p = .039$, $d = 1.37$, and the center midline VB, $t(19) = 4.53$, $p = .035$, $d = 1.37$, exhibited significantly greater alpha desynchronization than the posterior right VB.

Beta Band in Excitement Judgments. The analysis revealed a significant main effect of boundary type, $F(1, 19) = 39.34$, $p < .001$, $\eta_p^2 = .67$. This indicates that beta activity was greater for VB compared to HB. However, post hoc comparisons revealed a significantly greater beta power under HB compared to VB, $t(19) = 6.27$, $p < .001$, $d = 0.93$.

Additionally, there was a significant main effect of electrode location, $F(2, 38) = 12.40$, $p < .001$, $\eta_p^2 = .40$, suggesting that beta power varied topographically. Post hoc analyses indicated that posterior sites had significantly higher beta power compared to anterior, $t(19) = 4.46$, $p < .001$, $d = 0.44$, and central sites, $t(19) = 3.20$, $p = .014$, $d = 0.22$.

A significant main effect of hemisphere was also found, $F(2, 38) = 5.38$, $p = .009$, $\eta_p^2 = .22$. Post hoc comparisons showed that beta power in the left hemisphere was significantly lower than at the midline, $t(19) = -2.98$, $p = .023$, $d = -0.40$.

Furthermore, the interaction between Boundary Type × Electrode location was significant, $F(2, 38) = 16.41$, $p < .001$, $\eta_p^2 = .46$. Follow-up comparisons revealed that beta power was significantly higher in the anterior HB compared to the anterior VB, $t(19) = 3.56$, $p = .031$, $d = 0.54$, the center VB, $t(19) = 4.95$, $p = .001$, $d = 0.70$, and the posterior VB, $t(19) = 8.05$, $p < .001$, $d = 1.62$. Similarly, the posterior HB demonstrated greater beta activity than the anterior VB, $t(19) = 3.41$, $p = .044$, $d = 0.74$, the center VB, $t(19) = 3.96$, $p = .013$, $d = 0.90$, and the posterior VB, $t(19) = 5.80$, $p < .001$, $d = 1.83$. Additionally, the center VB showed significantly lower beta power than the posterior VB, $t(19) = 7.60$, $p < .001$, $d = 0.93$.

However, the interaction between Boundary Type × Hemisphere did not reach significance. A significant interaction between Electrode Location × Hemisphere was observed, $F(4, 76) = 3.25$, $p = .016$, $\eta_p^2 = .15$. Post hoc analyses revealed that beta power was significantly reduced at posterior left sites compared to the following locations: anterior midline, $t(19) = -4.04$, $p = .025$, $d = -1.08$, center midline, $t(19) = -4.14$, $p = .020$, $d = -0.98$, and anterior right, $t(19) = -4.20$, $p = .018$, $d = -1.10$. Additionally, beta activity at the anterior midline was significantly greater than that at the center right, $t(19) = 4.33$, $p = .013$, $d = 0.57$. Furthermore, beta power at the center midline was higher than at the center right, $t(19) = 3.95$, $p = .031$, $d = 0.46$, and the anterior right also showed grater beta power compared to the center right, $t(19) = 3.90$, $p = .034$, $d = 0.59$.

Lastly, the three-way interaction among boundary type, electrode location, and hemisphere was significant, $F(4, 76) = 10.78$, $p < .001$, $\eta_p^2 = .36$. Post hoc comparisons revealed that beta power in the anterior left VB was significantly greater in both the posterior left VB, $t(19) = 5.24$, $p = .007$, $d = 1.49$, and the posterior right VB, $t(19) = 6.37$, $p < .001$, $d = 1.93$. Similarly, beta power in the center left HB exceeded that of the posterior left VB, $t(19) = 4.54$, $p = .034$, $d = 1.75$, and the posterior right VB, $t(19) = 5.94$, $p = .003$, $d = 1.92$.

Furthermore, the anterior midline HB showed greater beta power than the center right HB, $t(19) = 4.72$, $p = .023$, $d = 0.84$, the center left VB, $t(19) = 4.51$, $p = .037$, $d = 0.91$, the posterior left VB, $t(19) = 6.73$, $p < .001$, $d = 1.63$, the posterior midline VB, $t(19) = 6.27$, $p < .001$, $d = 1.14$, and the posterior right VB, $t(19) = 8.52$, $p < .001$, $d = 2.07$.

In addition, the center midline HB showed greater beta power than the posterior left VB, $t(19) = 6.31$, $p < .001$, $d = 1.55$, the posterior midline VB, $t(19) = 5.89$, $p = .002$, $d = 1.06$, and the posterior right VB, $t(19) = 8.69$, $p < .001$, $d = 1.99$. The posterior midline HB was found to be higher than the posterior left VB, $t(19) = 5.07$, $p = .010$, $d = 1.92$, and the posterior right VB, $t(19) = 6.00$, $p = .001$, $d = 2.36$.

Moreover, the anterior right HB showed stronger beta power than the anterior left VB, $t(19) = 5.66$, $p = .007$, $d = 2.04$, and the posterior midline VB, $t(19) = 7.67$, $p < .001$, $d = 2.12$. The posterior right HB also surpassed the center left VB, $t(19) = 4.53$, $p = .035$, $d = 2.16$, the posterior left VB, $t(19) = 5.01$, $p = .012$, $d = 2.88$, the posterior midline VB, $t(19) = 4.43$, $p = .044$, $d = 2.39$, and finally, the posterior right VB, $t(19) = 6.18$, $p < .001$, $d = 3.33$.

The results indicated that the beta power in the posterior right VB was significantly greater than the anterior left VB, $t(19) = 6.95$, $p < .001$, $d = 1.35$. In contrast, the posterior left VB had significantly lower beta power than the anterior midline VB, $t(19) = -8.09$, $p < .001$, $d = -1.27$, center midline VB, $t(19) = -6.07$, $p = .001$, $d = -1.13$, anterior right VB, $t(19) = -5.03$, $p = .011$, $d = -1.14$, and center right VB, $t(19) = -4.89$, $p = .016$, $d = -0.97$. Additionally, the beta power in the posterior right VB was lower than that of the anterior midline VB, $t(19) = -9.53$, $p < .001$, $d = -1.71$, center midline VB, $t(19) = -8.47$, $p < .001$, $d = -1.58$, posterior midline VB, $t(19) = -5.60$, $p = .003$, $d = -0.93$, anterior right VB, $t(19) = -6.97$, $p < .001$, $d = -1.58$, and center right VB, $t(19) = -7.11$, $p < .001$, $d = -1.41$.

Theta Band in Excitement Judgments. The analysis revealed a significant interaction between Electrode Location × Hemisphere was observed, $F(2.92, 55.50) = 2.84$, $p = .048$, $\eta_p^2 = .13$. Despite this, no specific electrode–hemisphere combinations showed statistically significant effects, as their confidence intervals included zero. However, all other factors were nonsignificant. The results of repeated-measures ANOVAs conducted on alpha, beta, and theta power for the excitement judgments are presented in Table 2.

Oscillatory Activity in Fascination Judgments

Alpha Band in Fascination Judgments. The analysis revealed a significant main effect of boundary type, $F(1, 19) = 8.95$, $p = .007$, $\eta_p^2 = .32$. This indicates that alpha power differed significantly between the boundary types. Post hoc comparisons showed that alpha power was significantly greater for HB than VB, $t(19) = 4.40$, $p = .007$, $d = 0.98$. The main effect of electrode location was not significant.

However, a significant main effect of hemisphere was observed, $F(2, 38) = 9.89$, $p < .001$, $\eta_p^2 = .34$, suggesting that there are asymmetries in alpha oscillations across the hemispheres. Post hoc comparisons revealed that alpha power was significantly lower at the midline compared to the left hemisphere, $t(19) = -5.07$, $p = .004$, $d = 1.13$, and significantly higher at the midline compared to the right hemisphere, $t(19) = 3.31$, $p = .006$, $d = 0.74$.

Table 2
Repeated-Measures ANOVA Results for Alpha, Beta, and Theta Band Power in the Excitement Judgment

Excitement	Alpha	Beta	Theta
Boundary type	$\mathbf{F(1, 19) = 11.32, p = .003, \eta_p^2 = .37}$	$\mathbf{F(1, 19) = 39.34, p < .001, \eta_p^2 = .67}$	$F(1, 19) = 0.62$, $p = .442$
Electrode location	$\mathbf{F(1.45, 27.53) = 23.71, p < .001, \eta_p^2 = .55}$	$\mathbf{F(2, 38) = 12.40, p < .001, \eta_p^2 = .40}$	$F(2, 38) = 1.71$, $p = .195$
Hemisphere	$\mathbf{F(2, 25.38) = 7.04, p < .001, \eta_p^2 = .27}$	$\mathbf{F(2, 38) = 5.38, p = .009, \eta_p^2 = .22}$	$F(2, 38) = 0.66$, $p = .522$
Boundary Type × Electrode Location	$F(1.39, 26.48) = 1.92$, $p = .176$	$\mathbf{F(2, 38) = 16.41, p < .001, \eta_p^2 = .46}$	$F(2, 38) = 0.83$, $p = .444$
Boundary Type × Hemisphere	$\mathbf{F(1.33, 25.21) = 4.37, p = .037, \eta_p^2 = .19}$	$F(2, 38) = 2.95$, $p = .064$	$F(2, 38) = 0.21$, $p = .814$
Electrode Location × Hemisphere	$\mathbf{F(1.61, 30.52) = 7.72, p = .003, \eta_p^2 = .29}$	$\mathbf{F(4, 76) = 3.25, p = .016, \eta_p^2 = .15}$	$\mathbf{F(2.92, 55.50) = 2.84, p = .048, \eta_p^2 = .13}$
Boundary Type × Electrode Location × Hemisphere	$\mathbf{F(2.12, 40.34) = 4.70, p = .013, \eta_p^2 = .20}$	$\mathbf{F(4, 76) = 10.78, p < .001, \eta_p^2 = .36}$	$F(2.87, 54.56) = 0.83$, $p = .480$

Note. Bold values indicate statistically significant effects ($p < .05$). ANOVA = analysis of variance.

A significant interaction was found between Boundary Type × Electrode location, $F(1.07, 20.36) = 12.10$, $p = .002$, $\eta_p^2 = .39$. Alpha desynchronization was stronger at the posterior VB sites compared to the anterior VB, $t(19) = 7.11$, $p < .001$, $d = 1.59$, central VB, $t(19) = 4.80$, $p = .003$, $d = 1.07$, posterior HB, $t(19) = 4.62$, $p = .044$, $d = 1.03$, and central HB, $t(19) = 3.80$, $p = .018$, $d = 0.85$.

Additionally, the interaction between Boundary Type × Hemisphere was also significant, $F(1.29, 24.47) = 5.55$, $p = .030$, $\eta_p^2 = .23$, indicating lateralized effects of boundary conditions on alpha power. Post hoc tests showed that midline HB exhibited significantly lower alpha power compared to VB, $t(19) = 2.72$, $p = .041$, $d = 0.61$. Additionally, alpha power was significantly lower in the left HB compared to midline HB, $t(19) = -3.80$, $p = .007$, $d = 0.85$, while left VB, $t(19) = 3.48$, $p = .038$, $d = 0.78$, midline VB, $t(19) = 3.47$, $p = .038$, $d = 0.78$, and right VB, $t(19) = 3.72$, $p = .022$, $d = 0.83$, showed significantly higher alpha activity than midline HB. In contrast, the interaction between Electrode Location × Hemisphere was not significant.

Finally, the three-way interaction among boundary type, electrode location, and hemisphere was significant, $F(2.56, 48.72) = 6.70$, $p = .001$, $\eta_p^2 = .26$. This suggests that alpha activity was influenced by the combined effects of spatial electrode positioning, boundary configuration, and hemispheric organization. Post hoc comparisons revealed that posterior right VB showed significantly greater alpha power than posterior midline VB, $t(19) = 3.31$, $p = .046$, $d = 0.74$, central right VB, $t(19) = 3.74$, $p = .009$, $d = 0.84$, and anterior right VB, $t(19) = 3.47$, $p = .010$, $d = 0.78$. Posterior left VB exhibited significantly lower alpha power than anterior midline VB, $t(19) = -2.84$, $p = .031$, $d = 0.63$, and central midline VB, $t(19) = -3.11$, $p = .043$, $d = 0.70$. Additionally, posterior right VB showed significantly greater alpha power than central midline VB, $t(19) = 4.03$, $p = .048$, $d = 0.90$, and posterior midline VB, $t(19) = 4.08$, $p = .031$, $d = 0.91$. Further, center left VB was significantly lower than posterior left VB, $t(19) = -4.537$, $p = .035$, $d = -0.973$, and also showed reduced alpha power compared to center midline VB in two separate comparisons, $t(19) = -4.630$, $p = .028$, $d = -0.927$; $t(19) = -4.712$, $p = .023$, $d = -0.635$.

Beta Band in Fascination Judgments. The analysis revealed a significant main effect of boundary type, $F(1, 19) = 16.88$, $p = .001$, $\eta_p^2 = .47$, indicating that beta power significantly differed between HB and VB. Post hoc comparisons confirmed that VB elicited significantly greater beta activity than HB, $t(19) = 4.109$, $p < .001$, $d = 0.606$.

Additionally, a significant main effect of electrode location was observed, $F(2, 38) = 4.61$, $p = .016$, $\eta_p^2 = .20$, suggesting that beta oscillations varied across anterior, central, and posterior area. Post hoc analyses revealed that posterior sites exhibited significantly greater beta activity than anterior sites, $t(19) = -3.269$, $p = .012$, $d = -0.482$.

The main effect of hemisphere was also significant, $F(2, 38) = 18.08$, $p < .001$, $\eta_p^2 = .49$, reflecting hemispheric asymmetries in beta activity. Follow-up comparisons showed that beta power was significantly greater at midline electrodes compared to the left hemisphere sites, $t(19) = 5.354$, $p < .001$, $d = 0.498$. Additionally, beta power in the left hemisphere was significantly lower than that at the midline, $t(19) = -5.725$, $p < .001$, $d = -0.472$.

Furthermore, there was a significant interaction between Boundary Type × Electrode location, $F(1.30, 24.75) = 15.61$, $p < .001$, $\eta_p^2 = .45$. Post hoc comparisons indicated that posterior HB elicited significantly lower beta power than anterior HB, $t(19) = -4.099$, $p = .009$, $d = -1.461$, anterior VB, $t(19) = 4.442$, $p = .004$, $d = 1.242$, center VB, $t(19) = 3.790$, $p = .019$, $d = 1.290$, and posterior VB, $t(19) = 4.581$, $p = .003$, $d = 1.738$. Additionally, center HB showed a significantly lower beta power than posterior VB, $t(19) = 3.671$, $p = .024$, $d = 0.746$, while anterior VB exhibited greater beta power than posterior VB, $t(19) = 3.503$, $p = .036$, $d = 0.496$.

The interaction between Boundary Type × Hemisphere was also significant, $F(2, 38) = 7.43$, $p = .002$, $\eta_p^2 = .28$. Post hoc results revealed that midline HB was associated with greater beta activity than left VB, $t(19) = 5.770$, $p < .001$, $d = 0.942$, midline VB, $t(19) = 3.497$, $p = .036$, $d = 0.282$, and right VB, $t(19) = 5.859$, $p < .001$, $d = 1.078$. Additionally, right HB also showed greater beta power than left VB, $t(19) = 3.679$, $p = .024$, $d = 0.742$, and right VB, $t(19) = 4.290$, $p = .006$, $d = 0.877$. Moreover, left VB showed significantly lower beta activity than midline VB, $t(19) = -5.529$, $p < .001$, $d = -0.660$, while midline VB had greater activity than right VB, $t(19) = 5.517$, $p < .001$, $d = 0.795$.

An additional significant interaction was found between Electrode Location × Hemisphere, $F(2.74, 52.02) = 4.80$, $p = .006$, $\eta_p^2 = .20$. Post hoc analyses showed that the anterior left HB had significantly lower beta activity than the posterior left HB, $t(19) = -4.607$, $p = .029$, $d = -1.972$, the anterior midline HB, $t(19) = -5.128$, $p = .009$, $d = -1.216$, and the center midline HB, $t(19) = -5.290$, $p = .006$, $d = -1.276$. In contrast, the anterior left VB showed significantly greater beta activity than both the center left VB, $t(19) = 4.453$, $p = .042$, $d = 1.046$, and the posterior left VB, $t(19) = 4.443$, $p = .016$, $d = 0.936$. Additionally, the posterior right HB exceeded both the anterior right VB, $t(19) = 4.616$, $p = .029$, $d = 1.819$, and the posterior right VB, $t(19) = 4.621$, $p = .029$, $d = 2.707$.

Finally, the three-way interaction among boundary type, electrode location, and hemisphere was significant, $F(1.89, 35.83) = 6.06$, $p = .006$, $\eta_p^2 = .24$, indicating that beta oscillatory dynamics were influenced by the combined effects of spatial configuration and hemispheric lateralization. Post hoc comparisons showed that within the midline VB sites, the anterior midline showed significantly lower activity compared to both the anterior midline, $t(19) = -5.085$, $p = .010$, $d = -0.843$, and the center midline, $t(19) = -4.550$, $p = .034$, $d = -0.797$. Additionally, center midline VB was significantly higher than that of the posterior midline VB, $t(19) = 5.132$, $p = .009$, $d = 1.472$, and the posterior right VB, $t(19) = 5.176$, $p = .008$, $d = 1.427$. Moreover, the posterior midline VB was also greater than that of the posterior right VB, $t(19) = 4.767$, $p = .021$, $d = 1.002$. Furthermore, center left VB showed significantly lower activity compared to posterior left VB, $t(19) = -4.537$, $p = .035$, $d = -0.973$, and was also lower than the center midline VB in two separate comparisons, $t(19) = -4.630$, $p = .028$, $d = -0.927$; $t(19) = -4.712$, $p = .023$, $d = -0.635$.

Theta Band in Fascination Judgments. The analysis found all factors were nonsignificant. The results of repeated-measures ANOVAs conducted on alpha, beta, and theta power for the fascination judgments are presented in Table 3.

The modulation of oscillatory activity based on architectural boundary type during aesthetic judgments is illustrated in Figure 10.

Table 3
Repeated-Measures ANOVA Results for Alpha, Beta, and Theta Band Power in the Fascination Judgment

Fascination	Alpha	Beta	Theta
Boundary type	**$F(1, 19) = 8.95, p = .007, \eta_p^2 = .32$**	**$F(1, 19) = 16.88, p = .001, \eta_p^2 = .47$**	$F(1, 19) = 2.44, p = .135$
Electrode location	$F(1.30, 24.67) = 2.62, p = .111$	**$F(2, 38) = 4.61, p = .016, \eta_p^2 = .20$**	$F(2, 38) = 3.24, p = .050, \eta_p^2 = .15$
Hemisphere	**$F(2, 38) = 9.89, p < .001, \eta_p^2 = .34$**	**$F(2, 38) = 18.08, p < .001, \eta_p^2 = .49$**	$F(1.38, 26.25) = 0.23, p = .710$
Boundary Type × Electrode Location	**$F(1.07, 20.36) = 12.10, p = .002, \eta_p^2 = .39$**	**$F(1.30, 24.75) = 15.61, p < .001, \eta_p^2 = .45$**	$F(2, 38) = 0.28, p = .756$
Boundary Type × Hemisphere	**$F(1.29, 24.47) = 5.55, p = .030, \eta_p^2 = .23$**	**$F(2, 38) = 7.43, p = .002, \eta_p^2 = .28$**	$F(2, 38) = 0.97, p = .389$
Electrode Location × Hemisphere	$F(2.09, 39.68) = 2.05, p = .140$	**$F(2.74, 52.02) = 4.80, p = .006, \eta_p^2 = .20$**	$F(1.82, 34.65) = 2.02, p = .151$
Boundary Type × Electrode Location × Hemisphere	**$F(2.56, 48.72) = 6.70, p = .001, \eta_p^2 = .26$**	**$F(1.89, 35.83) = 6.06, p = .006, \eta_p^2 = .24$**	$F(4, 76) = 0.95, p = .439$

Note. Bold values indicate statistically significant effects ($p < .05$). ANOVA = analysis of variance.

This figure presents the mean power values in the alpha, beta, and theta frequency bands for vertical and horizontal boundaries. The data is displayed separately for midline electrode sites: frontal (Fz), central (Cz), parietal (Pz), and occipital (Oz), allowing us to capture area-specific neural dynamics. This visualization offers insight into how distinct cortical areas respond to architectural features during aesthetic evaluations. Additional figures that illustrate the interactions among boundary type, hemisphere, and cortical area are provided in Appendix.

Discussion

This study explored the oscillatory dynamics underlying three dimensions of aesthetic judgment: familiarity, excitement, and fascination (Elver Boz et al., 2024a). It focused on various architectural variables, including curvilinear boundaries, color, light, texture, and size. Using EEG, the researchers recorded changes in neural activity alongside ratings for the three aesthetic dimensions ratings. The rhythmic patterns of neural activity, known as brain oscillations, were captured through ERSPs, providing a time-resolved measure of electrocortical dynamics associated with stimulus processing. These patterns are temporally sensitive and indicate variations in arousal, perception, and cognitive function in response to different architectural variables (Azzazy et al., 2021; Bell & Cuevas, 2012).

Effects of Architectural Variables on Aesthetic Judgments in Behavioral Data

The findings indicate that people perceived HB as more familiar and VB as more exciting and fascinating, replicating the results of Elver Boz et al. (2024b). Since individuals spend most of their time in interior spaces, the influence of modern architecture has increased familiarity with HB differences. These spaces are viewed as "familiar-known spaces" because they resemble traditional 90-degree designs. In contrast, VB are rarely seen in modern architecture, often representing distinctive structures or signature buildings. Consequently, VB are perceived as "exciting" and "fascinating." The primary focus of this study was to explore the relationship between behavioral data and neural responses.

Effects of Architectural Variables on Aesthetic Judgments in Neural Data

To gain better understanding of the temporal dynamics of aesthetic experience, the study employed time–frequency analysis of EEG data using ERSPs. ERSPs provided insights into the functional role of oscillatory activity across frequency bands by capturing both synchronization (increased power) and desynchronization (reduced power). These changes are believed to reflect various cognitive and affective states (Makeig et al., 1996). The EEG analysis indicated that alpha and beta oscillations were significantly modulated by both boundary type and spatial location, particularly in posterior and hemispheric areas. This suggests that these oscillations play a role in attentional allocation and perceptual fluency when assessing aesthetic judgements of familiarity, excitement, and fascination. However, theta oscillations showed notable modulation only for familiarity judgements, potentially reflecting the mnemonic and spatial encoding challenges posed by the more novel VB stimuli, as indicated by the behavioral data. The

Figure 10

Illustrates the Oscillatory Activity in the Alpha, Beta, and Theta Bands for Vertical and Horizontal Boundaries, Across the Aesthetic Judgment Task, Separately Depicted for the Midline Fz, Cz, Pz, and Oz Areas

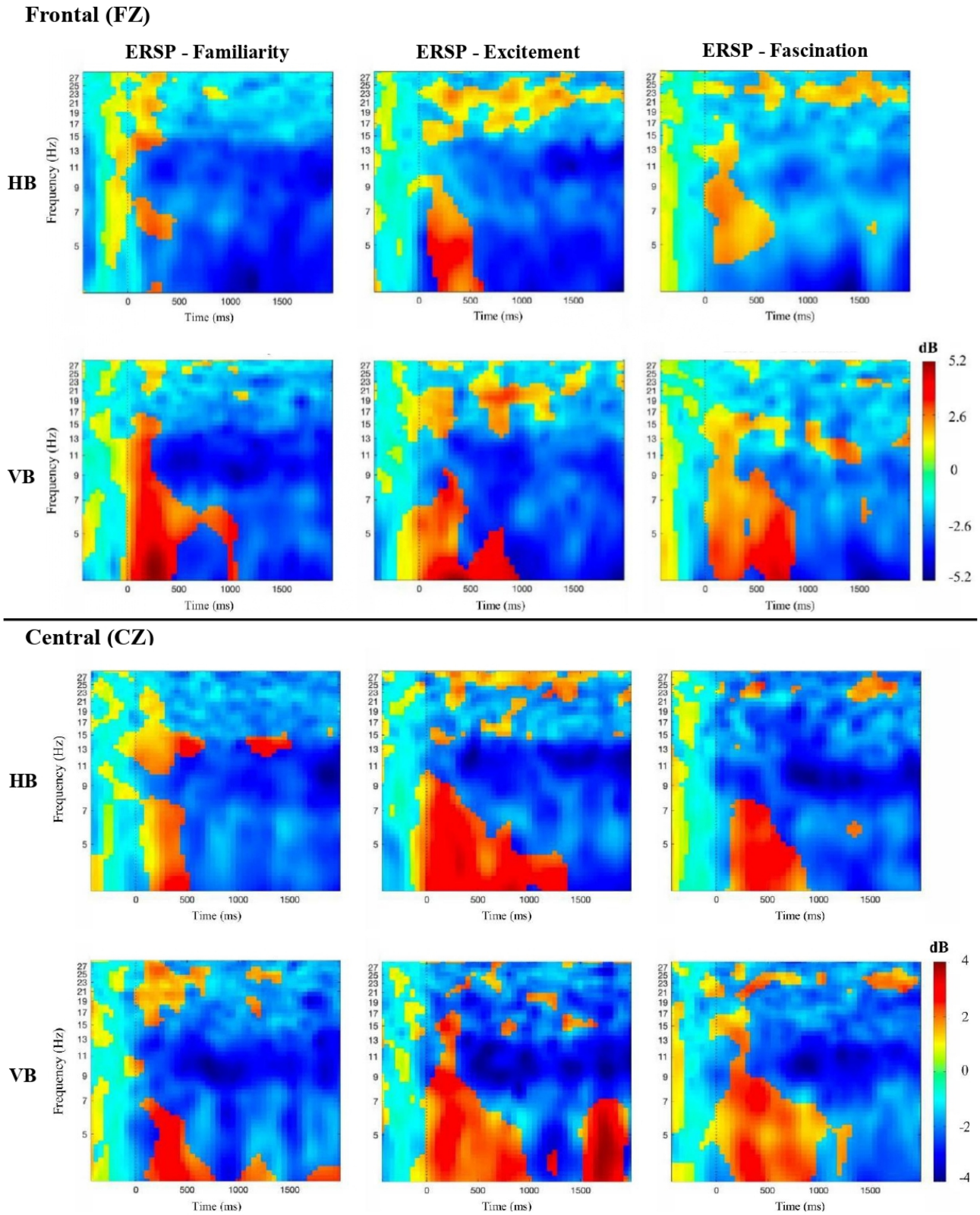

(*figure continues*)

Figure 10 *(continued)*

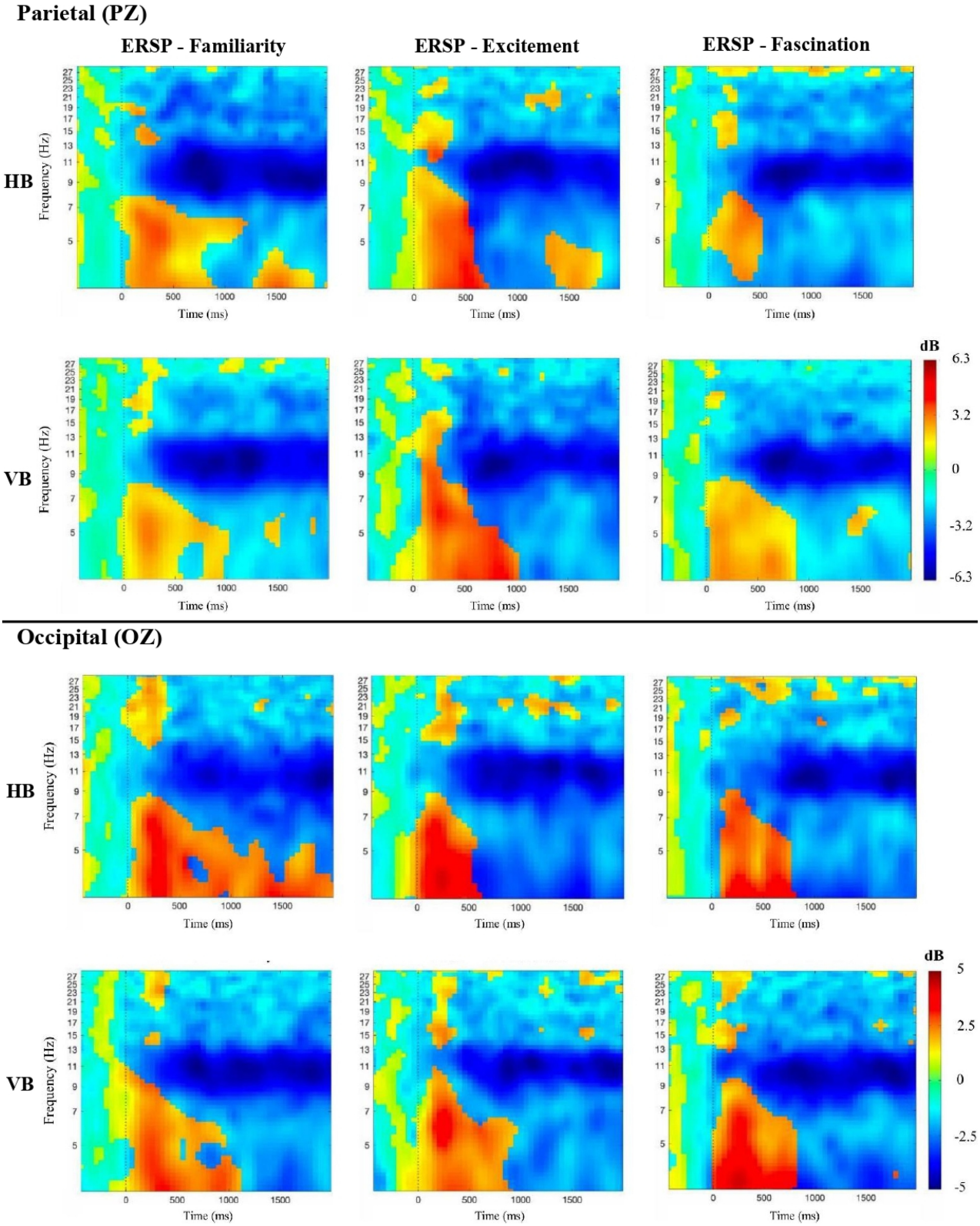

Note. HB = horizontal boundaries; VB = vertical boundaries; ERSP = event-related spectral perturbation; dB = decibel; Fz = frontal; Cz = central; Pz = parietal; Oz = occipital. See the online article for the color version of this figure.

following sections detail the distinct contributions of each frequency band to aesthetic judgments.

Alpha Oscillations and Aesthetic Judgments

Alpha Oscillations in Familiarity Judgments. There is stronger alpha desynchronization in posterior areas and VB. The alpha desynchronization, often interpreted as increased cortical activation, suggests heightened perceptual and attentional engagement (Jensen & Mazaheri, 2010; Klimesch, 1999). It indicates enhanced perceptual and attentional processing in posterior area during VB processing when familiarity is perceived. The main effect observed at different electrode locations implies a dominance of alpha desyncronization in the posterior areas, reflecting the engagement of occipital and parietal networks that are responsible for spatial perception and scene analysis. The stronger alpha suppression elicited by VB suggests that these boundaries heighten the demands for sensory processing.

Further post hoc analysis revealed interactions among electrode location and boundary types, hemisphere and boundary, as well as a three-way interaction between spatial topography, hemisphere, and boundary. The findings showed that there was greater alpha desynchronization in the posterior area for VB compared to HB, which aligns with the role of posterior visual cortex in processing environmental form and familiarity. Additionally, the hemispheric effects indicated that the midline and right hemisphere were more involved in processing VB, suggesting a possible specialization of the right hemisphere for processing environmental novelty, such as VB.

Three-way interactions indicate a spatialized and lateralized pattern, with the strongest alpha suppression observed in the posterior right area and the midline under VB. This finding supports theories of lateralized spatial coding. It aligns with the notion that alpha oscillations indicate cortical idling and the suppression of irrelevant stimuli, which helps facilitate focused attention (Foxe & Snyder, 2011). The increased alpha suppression in occipital and parietal cortices may enhance the prioritization of environmental features for aesthetic evaluation, especially in situations involving spatial novelty.

Alpha Oscillations in Excitement Judgments. Boundary type, electrode location, and hemisphere were found to influence excitement judgements. Specifically, VB elicited greater alpha desynchronization compared to HB, suggesting increased cognitive or perceptual engagement during the evaluations.

Alpha power varied across different brain locations, with posterior sites showing greater alpha power (indicating synchronization) than anterior and central area. This finding may emphasize the role of occipital areas in excitement judgments, potentially reflecting a disengagement from external sensory input or inhibitory control during emotionally arousing excitement evaluations (N. R. Cooper et al., 2003; Foxe & Snyder, 2011; Klimesch, 2012). Additionally, alpha activity differed by hemisphere, with midline sites displaying stronger activity than the right hemisphere area.

Further interactions indicated that alpha desynchronization was more pronounced in the right hemisphere under VB compared to both the left and midline hemispheres under HB and VB. This suggests that the right hemisphere is more sensitive to VB forms when they are emotionally salient (Davidson & Irwin, 1999).

Posterior right electrodes revealed the highest levels of alpha power, exceeding most other areas, which reflects area-specific processing of emotionally salient environmental forms. Three-way comparisons indicated that the posterior left area showed greater desynchronization under VB than various other conditions, such as center right HB, anterior left VB, and posterior right HB. This divergence may indicate a division of labor across the hemispheres: The left posterior cortex likely supports scene parsing and attentional reorientation, while the right hemisphere may play a more prominent role in affective modulation and sensory gating. These findings align with prior research demonstrating the link between alpha activity, enhanced attention, and reduced distraction during visual tasks (Buschman & Miller, 2007), as well as the role of alpha oscillations in processing emotionally salient stimuli (Knyazev, 2007).

Alpha Oscillations in Fascination Judgments. Boundary type and hemisphere influenced alpha power. Alpha power was lower for VB compared to HB, indicating greater alpha desynchronization. Additionally, at midline sites, alpha power was lower than in the left hemisphere but higher than in the right hemisphere, suggesting a higher engagement of the right hemisphere. The interaction between boundary type and electrode location underlines that posterior areas under VB show stronger alpha desynchronization than both anterior and central areas under VB, as well as posterior and central areas under HB. Hemispheric differences indicate lateralized processing, with the left hemisphere showing more alpha suppression under VB.

Three-way comparisons indicate that the posterior right VB area shows the strongest synchronization, while the posterior left VB shows strong desynchronization. This proposes that the posterior left and right area have diverging functions, implying a specialization: The left area may be involved in scene processing and active external attention, whereas the right area appears to focus on perceptual attention, inhibiting external stimuli. These findings are consistent with previous research linking alpha activity in central parietal areas to the visual processing of architectural features (Jensen & Mazaheri, 2010; Klimesch, 1999). They also support the idea that alpha rhythms facilitate attention by suppressing distractions.

Overall, alpha oscillations were found to play a key role across three dimensions of aesthetic experience, reflecting changes in attentional focus, perceptual processing, and cortical engagement. Familiarity judgments resulted in notable alpha desynchronization in the posterior and right midline area under VB conditions, indicating enhanced visual and spatial processing in response to environmental novelty. Excitement was associated with stronger desynchronization under VB, particularly in the left posterior area, while HB showed greater synchronization, suggesting a distinction between external sensory engagement and internally stabilized evaluation.

Fascination exhibited increased desynchronization under VB in posterior and midline areas, whereas synchronization was observed in anterior and right hemispheric area. This reflects a dynamic interplay between attentional filtering and embodied simulation. These patterns indicate that alpha modulation supports both bottom-up sensory processing and top-down attentional control, with spatial and hemispheric specificity that mirrors the complexity of aesthetic appraisal in built environments (Foxe & Snyder, 2011; Klimesch, 1999; Knyazev, 2007).

Beta Oscillations and Aesthetic Judgements

Beta Oscillations in Familiarity Judgments. Beta power varied according to architectural boundary type, electrode location, and

hemisphere. VB elicited greater beta desynchronization, which is reflected by a reduction in synchronization within the beta frequency band. This desynchronization is often interpreted as a neural marker of active information processing, including increased environmental awareness, spatial evaluation, and readiness for interaction.

Analysis of the three-way interaction revealed that VB-specific activation occurred in posterior midline and right frontal area, indicating that curvature acts as a topographically specific stimulus. The beta desynchronization in response to VB was particularly pronounced in posterior and midline area, suggesting involvement of sensorimotor integration and attentional networks. The consistent observation of the strongest desynchronization in the posterior right and midline VB conditions implies that these areas are especially sensitive to curvilinear architectural features.

These results support theoretical models suggesting that curved spaces may enhance perceptual fluency or embodied simulation, which in turn modulates underlying beta oscillatory activity as participants process environmental familiarity (Leder et al., 2004).

Beta Oscillations in Excitement Judgments. Beta oscillations varied according to boundary type, electrode location, and hemisphere. Higher beta synchronization was observed in HB, indicating a more stable engagement in sensorimotor processing in HB. Additionally, posterior sites displayed greater beta synchronization, which may be associated with visual–spatial integration. Midline electrodes also showed higher synchronization compared to lateral electrodes, further reflecting integrative processing.

The comparison of interactions noted that beta activity showed stronger synchronization under HB, especially at the anterior and posterior sites. This suggests greater cognitive stability for HB. In contrast, the central VB sites showed reduced synchronization. An analysis of hemispheric patterns indicated desynchronization in the posterior left area, while the midline and right anterior/central sites showed higher beta power, indicating lateralized processing.

Three-way interactions revealed that the anterior left hemisphere showed desynchronization compared to the posterior and midline area. Under VB, the anterior left showed more synchronization than the posterior VB. Notably, the posterior right VB showed the strongest desynchronization, suggesting it is especially sensitive to VB. These findings are consistent with previous research linking beta activity in the occipital and parietal areas to emotionally arousing and visually stimulating experiences (Chatterjee & Vartanian, 2014. This suggests that excitement involves both sensorimotor coordination and affective–motivational appraisal, with beta synchronization marking stable attention and desynchronization indicating active perceptual exploration.

Beta Oscillations in Fascination Judgments. Beta oscillations varied according to boundary type, electrode location, and hemisphere. VB yielded greater beta synchronization compared to HBs, indicating a higher level of top-down control and engagement with the stimuli. Posterior areas showed greater beta synchronization, reflecting enhanced perceptual and evaluative processing in occipital and/or parietal areas in processing architectural stimuli. These findings are consistent with the idea that visual analysis and decision-related processes are fundamental to feelings of fascination (Engel et al., 2001). Additionally, the midline areas exhibited greater synchronization than the lateral sides, suggesting greater engagement of central cortical areas.

Posterior area under HB conditions showed beta desynchronization, which may indicate increased engagement with spatial features in those settings. This pattern suggests that fascination perception under HB requires greater cognitive effort for processing. In contrast, under VB, anterior area, particularly in the left hemisphere, exhibited heightened beta synchronization. This may indicate a more internally stabilized state, where the environment feels coherent or familiar, resulting in less need for active perceptual reorganization. Previous literature links activation in the left hemisphere to emotionally rich stimuli and semantic elaboration (Davidson & Irwin, 1999), which may explain this observed pattern. The three-way interaction highlighted that anterior left area exhibited strong desynchronization under HB, whereas the same areas showed synchronized activity under VB. This finding emphasizes the shifting processing modes depending on the spatial context.

Overall, beta oscillations were found to play a key role across all three aesthetic dimensions, though the direction and localization of their effects varied. Familiarity was associated with desynchronization in the posterior midline VB area, indicating a dynamic interaction with spatial cues. Excitement involved beta synchronization under HB and desynchronization under VB, especially in the lateralized posterior area, reflecting a balance between attentional engagement and perceptual fluency. Fascination showed higher beta synchronization under VB and a more variable pattern under HB, suggesting different levels of evaluative effort and emotional resonance. The lateralized beta activity across hemispheres—especially in the occipital and parietal area—supports a differentiated processing architecture for aesthetic experiences, integrating both visual analysis and emotional meaning making (Corbetta & Shulman, 2002; Salinas & Sejnowski, 2001).

Theta Oscillations and Aesthetic Judgements

Theta Oscillations in Familiarity Judgments. Theta band power was higher for VB, which is often associated with memory encoding, spatial attention, and cognitive effort, particularly when the stimuli are less familiar or require active cognitive processing (Busch & Herrmann, 2003; Klimesch, 1999; Summerfield & Mangels, 2005). This observation aligns with the finding that VB were perceived as less familiar than HB. Additionally, prior studies suggest that decreases in theta may indicate reduced memory demand (Klimesch, 1999).

Aside from boundary effects, several interaction effects suggest the presence of spatialized theta activity. The central and posterior area under VB were higher in theta power compared to anterior areas and HB. Notably, strong interactions were observed in the center-left, center-midline, and center-right areas. The three-way comparisons highlighted that VB seemed to enhance theta activity in the central areas, as well as in left hemisphere and midline area.

Theta Oscillations in Excitement and Fascination Judgments. The results revealed no clear effects of theta band oscillations on judgments of excitement or fascination. This suggests that theta oscillations may not play a central role in these specific aesthetic perceptions, at least within the context of the spatial and perceptual demands of the current task. Instead, cognitive and affective processes related to excitement and fascination may be more closely associated with alpha and beta band dynamics, which reflect attentional modulation and sensorimotor engagement.

Relationships Between Aesthetic Judgments Across Behavioral and Neural Data

When the study examined how people responded to different architectural spaces, both in their behavioral responses and in their neural activity, it revealed interesting overlaps as well as clear differences between the three aesthetic dimensions; familiarity, excitement, and fascination. Participants generally found HB more familiar, whereas VB tended to trigger stronger feelings of excitement and fascination. This makes intuitive sense: HB are what people encounter most often in daily life as simple and predictable. VB, on the other hand, tend to stand out. Their uncommon shapes and visual intensity make them more emotionally engaging.

These subjective impressions were also reflected in neural activity. When participants judged how familiar a space felt, there were noticeable changes across all three brainwave types (alpha, beta, and theta) especially in response to VB. This combination of brainwave patterns, particularly in the posterior and midline regions, refer to greater mental effort: The brain may be trying to make sense of an unfamiliar form by drawing on memory, directing attention, and actively processing spatial features. So, it seems that familiarity is not instic feeling—it is something the brain works to figure out—especially when the space does not match what we usually expect.

Things looked different with excitement and fascination. These feelings were not tied to theta waves, which often relate to memory. Instead, changes appeared mainly in the alpha and beta bands. Both excitement and fascination led to stronger alpha desynchronization and beta synchronization under VB—especially in the back of the brain and on the right side. This pattern fits with what we know about visual attention and emotional arousal: When a space is visually rich and unexpected, it grabs our attention and stirs something emotionally.

While excitement and fascination followed a similar neural path, they were not identical. Fascination seemed to involve a bit more variation between the two brain hemispheres, possibly pointing to a more emotionally immersive or even self-reflective experience.

All in all, these findings suggest that while all three judgments—familiarity, excitement, and fascination—draw on how we perceive and attend to space, they do not rely on the same mental systems. Familiarity pulls more from memory and spatial recognition. Excitement and fascination, on the other hand, lean into affective and sensory responses. Even in the same environment, the way we experience architecture can take very different routes in the brain.

Further Directions and Limitations

Further research must address neural patterns' cultural and personal variations, providing information into the universality or variability of aesthetic judgments (Leder et al., 2004). Longitudinal studies that examine the link between exposure to an architectural design and aesthetic judgments may reveal the impact of architectural design on human perception and well-being (Chatterjee & Vartanian, 2014. Building on the stimuli utilized in the present study and the implications of the observed neural patterns, future research should aim to pinpoint how different and more complex architectural forms might evoke specific aesthetic experiences (Chatterjee, 2011).

It should be noted that the present study design lacks a baseline measure, during which participants did not engage in aesthetic perception. This baseline is important for comparing neural activations during aesthetic judgment tasks, as it may help distinguish task-specific neural responses from the baseline brain activity when exposed to architectural variables (Handy, 2005; Plichta et al., 2012). With an appropriate baseline, it would be easier to isolate neural patterns that are directly related to aesthetic evaluation (Ashby & Helie, 2011). Future studies should include baseline neural activity measurements alongside aesthetic judgment tasks and adopt open science practices such as preregistration to enhance transparency. While the current study has sufficient statistical power, conducting a priori power analyses can help reduce researcher degrees of freedom (Nosek et al., 2018; Simmons, Nelson, & Simonsohn, 2011). Increasing the sample size would also improve the statistical power and generalizability of the findings (Button et al., 2013). Moreover, if EEG is used, integrating source localization techniques (e.g., sLORETA, beamforming) could provide more precise insights into the cortical generators involved in aesthetic processing (Michel & Brunet, 2019; Pascual-Marqui, 2002).

Another important point to note is that even though EEG is superior in capturing temporal changes in brain activity, it falls short in spatial resolution, meaning it cannot capture specific brain regions involved in aesthetic judgments (Buzsáki & Draguhn, 2004; Cohen, 2014; Luck, 2014; Michel et al., 2004). Therefore, fMRI studies are encouraged to elucidate specific brain regions associated with aesthetic judgments, given that fMRI can localize active brain regions with much higher spatial resolution than EEG (Huettel et al., 2014; Logothetis, 2008). By capturing detailed information about which brain areas are involved in processing aesthetic experiences, fMRI could offer insights that complement the temporal precision provided by EEG (Ogawa et al., 1993).

Conclusion

The findings of this study provide insight into the behavioral and neural basis of architectural aesthetic judgments. In terms of behavior, participants gave VB greater ratings for excitement and intrigue while ranking HB as more familiar. The neural results indicated that alpha oscillations revealed greater desynchronization for VB compared to HB. Additionally, lateralized beta activity for VB during aesthetic judgement suggests that verticality in architecture may enhance visual and emotional engagement (Ryu & Myung, 2005). Other hand, the relationship between theta synchronization and memory encoding for VB when valuating familiarity aligns with the observation that HB generally perceived as more familiar. In terms of neural aspect, higher beta and alpha activity for VB, as opposed to HB, suggests that the verticality in architecture may support visual and emotional engagement (Ryu & Myung, 2005).

References

Adams, M. (2013). Quality of urban spaces and wellbeing. In R. Cooper, E. Burton, & C. L. Cooper (Eds.), *Wellbeing and the environment* (Vol. 2, pp. 249–270). John Wiley & Sons. https://doi.org/10.1002/9781118539415.wbwell064

Ashby, F. G., & Helie, S. (2011). A tutorial on computational cognitive neuroscience: Modeling the neurodynamics of cognition. *Journal of Mathematical Psychology*, *55*(4), 273–289. https://doi.org/10.1016/j.jmp.2011.04.003

Azzazy, S., Ghaffarianhoseini, A., GhaffarianHoseini, A., Naismith, N., & Doborjeh, Z. (2021). A critical review on the impact of built environment

on users' measured brain activity. *Architectural Science Review*, *64*(4), 319–335. https://doi.org/10.1080/00038628.2020.1749980

Banaei, M., Ahmadi, A., & Yazdanfar, A. (2017). Application of AI methods in the clustering of architecture interior forms. *Frontiers of Architectural Research*, *6*(3), 360–373. https://doi.org/10.1016/j.foar.2017.05.002

Banaei, M., Hatami, J., Yazdanfar, A., & Gramann, K. (2017). Walking through architectural spaces: The impact of interior forms on human brain dynamics. *Frontiers in Human Neuroscience*, *11*, Article 477. https://doi.org/10.3389/fnhum.2017.00477

Bell, M. A., & Cuevas, K. (2012). Using EEG to study cognitive development: Issues and practices. *Journal of Cognition and Development*, *13*(3), 281–294. https://doi.org/10.1080/15248372.2012.691143

Brooks, J. L., Sala, S. D., & Logie, R. H. (2011). Tactile rod bisection in the absence of visuo-spatial processing in children, mid-age and older adults. *Neuropsychologia*, *49*(12), 3392–3398. https://doi.org/10.1016/j.neuropsychologia.2011.08.015

Busch, N. A., & Herrmann, C. S. (2003). Object-load and feature-load modulate EEG in a short-term memory task. *Neuroreport*, *14*(13), 1721–1724. https://doi.org/10.1097/00001756-200309150-00013

Buschman, T. J., & Miller, E. K. (2007). Top-down versus bottom-up control of attention in the prefrontal and posterior parietal cortices. *Science*, *315*(5820), 1860–1862. https://doi.org/10.1126/science.1138071

Button, K. S., Ioannidis, J. P., Mokrysz, C., Nosek, B. A., Flint, J., Robinson, E. S., & Munafò, M. R. (2013). Power failure: Why small sample size undermines the reliability of neuroscience. *Nature Reviews Neuroscience*, *14*(5), 365–376. https://doi.org/10.1038/nrn3475

Buzsáki, G., & Draguhn, A. (2004). Neuronal oscillations in cortical networks. *Science*, *304*(5679), 1926–1929. https://doi.org/10.1126/science.1099745

Cela-Conde, C. J., Marty, G., Maestú, F., Ortiz, T., Munar, E., Fernández, A., Roca, M., Rosselló, J., & Quesney, F. (2004). Activation of the prefrontal cortex in the human visual aesthetic perception. *Proceedings of the National Academy of Sciences*, *101*(16), 6321–6325. https://doi.org/10.1073/pnas.0401427101

Chatterjee, A. (2004a). Prospects for a cognitive neuroscience of visual aesthetics. *Bulletin of Psychology and the Arts*, *4*(2), 56–60. https://doi.org/10.1037/e514602010-003

Chatterjee, A. (2004b). The neuropsychology of visual artistic production. *Neuropsychologia*, *42*(11), 1568–1583. https://doi.org/10.1016/j.neuropsychologia.2004.03.011

Chatterjee, A. (2011). Neuroaesthetics: A coming of age story. *Journal of Cognitive Neuroscience*, *23*(1), 53–62. https://doi.org/10.1162/jocn.2010.21457

Chatterjee, A. (2013). *The aesthetic brain: How we evolved to desire beauty and enjoy art*. Oxford University Press. https://doi.org/10.1093/acprof:oso/9780199811809.001.0001

Chatterjee, A., & Vartanian, O. (2014). Neuroaesthetics. *Trends in Cognitive Sciences*, *18*(7), 370–375. https://doi.org/10.1016/j.tics.2014.03.003

Chatterjee, A., & Vartanian, O. (2016). Neuroscience of aesthetics. *Annals of the New York Academy of Sciences*, *1369*(1), 172–194. https://doi.org/10.1111/nyas.13035

Coburn, A., Vartanian, O., & Chatterjee, A. (2017). Buildings, beauty, and the brain: A neuroscience of architectural experience. *Journal of Cognitive Neuroscience*, *29*(9), 1521–1531. https://doi.org/10.1162/jocn_a_01146

Coburn, A., Vartanian, O., Kenett, Y. N., Nadal, M., Hartung, F., Hayn-Leichsenring, G., Navarrete, G., González-Mora, J. L., & Chatterjee, A. (2020). Psychological and neural responses to architectural interiors. *Cortex*, *126*, 217–241. https://doi.org/10.1016/j.cortex.2020.01.009

Cohen, M. X. (2014). *Analyzing neural time series data: Theory and practice*. MIT Press.

Color-blindness.com. (2023). *Ishihara 38 plates CVD test-Colblindor*. https://www.color-blindness.com/ishihara-38-plates-%20cvd-test/#prettyPhoto.

Cooper, N. R., Croft, R. J., Dominey, S. J., Burgess, A. P., & Gruzelier, J. H. (2003). Paradox lost? Exploring the role of alpha oscillations during externally vs. internally directed attention and the implications for IDA. *International Journal of Psychophysiology*, *47*(1), 65–74. https://doi.org/10.1016/S0167-8760(02)00107-1

Cooper, R., Burton, E., & Cooper, C. L. (Eds.) (2014). *Wellbeing and the environment*. John Wiley & Sons.

Corbetta, M., & Shulman, G. L. (2002). Control of goal-directed and stimulus-driven attention in the brain. *Nature Reviews Neuroscience*, *3*(3), 201–215. https://doi.org/10.1038/nrn755

Davidson, R. J., & Irwin, W. (1999). The functional neuroanatomy of emotion and affective style. *Trends in Cognitive Sciences*, *3*(1), 11–21. https://doi.org/10.1016/S1364-6613(98)01265-0

Delorme, A., & Makeig, S. (2004). EEGLAB: An open source toolbox for analysis of single-trial EEG dynamics. *Journal of Neuroscience Methods*, *134*(1), 9–21. https://doi.org/10.1016/j.jneumeth.2003.10.009

Di Dona, G., & Ronconi, L. (2023). Beta oscillations in vision: A (preconscious) neural mechanism for the dorsal visual stream? *Frontiers in Psychology*, *14*, Article 1296483. https://doi.org/10.3389/fpsyg.2023.1296483

Dobkins, K. R., & Heyman, G. D. (2013). Using neuroscience and behavioural data to tailor visual environments for infants and children. *Intelligent Buildings International*, *5*(sup1), 79–93. https://doi.org/10.1080/17508975.2013.817324

Donner, T. H., & Siegel, M. (2011). A framework for local cortical oscillation patterns. *Trends in Cognitive Sciences*, *15*(5), 191–199. https://doi.org/10.1016/j.tics.2011.03.007

Dzebic, V., Perdue, J. S., & Ellard, C. G. (2013). The influence of visual perception on responses towards real-world environments and application towards design. *Intelligent Buildings International*, *5*(sup1), 29–47. https://doi.org/10.1080/17508975.2013.807766

Eberhard, J. P. (2009). *Brain landscape: The coexistence of neuroscience and architecture*. Oxford University Press.

Elver Boz, T., Demirkan, H., & Urgen, B. A. (2024a). Visual perception of the built environment in virtual reality: A systematic characterization of human aesthetic experience in spaces with curved boundaries. *Psychology of Aesthetics, Creativity, and the Arts*, *18*(6), 1043–1058. https://doi.org/10.1037/aca0000504

Elver Boz, T., Demirkan, H., & Urgen, B. A. (2024b). The aesthetic experience of interior spaces with curvilinear boundaries and various space properties in immersive and desktop-based virtual environments. *Psychology of Aesthetics, Creativity, and the Arts*. Advance online publication. https://doi.org/10.1037/aca0000723

Engel, A. K., & Fries, P. (2010). Beta-band oscillations—Signalling the status quo? *Current Opinion in Neurobiology*, *20*(2), 156–165. https://doi.org/10.1016/j.conb.2010.02.015

Engel, A. K., Fries, P., & Singer, W. (2001). Dynamic predictions: Oscillations and synchrony in top-down processing. *Nature Reviews Neuroscience*, *2*(10), 704–716. https://doi.org/10.1038/35094565

Faul, F., Erdfelder, E., Lang, A.-G., & Buchner, A. (2007). G*Power 3: A flexible statistical power analysis program for the social, behavioral, and biomedical sciences. *Behavior Research Methods*, *39*(2), 175–191. https://doi.org/10.3758/BF03193146

Foxe, J. J., & Snyder, A. C. (2011). The role of alpha-band brain oscillations as a sensory suppression mechanism during selective attention. *Frontiers in Psychology*, *2*, Article 154. https://doi.org/10.3389/fpsyg.2011.00154

Gifford, R. (2002). *Environmental psychology: Principles and practice*. Optimal Books.

Handy, T. C. (2005). *Event-related potentials: A methods handbook*. MIT Press.

Hanslmayr, S., Spitzer, B., & Bäuml, K.-H. T. (2009). Brain oscillations dissociate between semantic and nonsemantic encoding of episodic memories. *Cerebral Cortex*, *19*(7), 1631–1640. https://doi.org/10.1093/cercor/bhn197

Hartig, T. (2008). Green space, psychological restoration, and health inequality. *The Lancet*, *372*(9650), 1614–1615. https://doi.org/10.1016/S0140-6736(08)61669-4

Huettel, S. A., Song, A. W., & McCarthy, G. (2014). *Functional magnetic resonance imaging* (3rd ed.). Sinauer Associates.

Jelić, A., Tieri, G., De Matteis, F., Babiloni, F., & Vecchiato, G. (2016). The enactive approach to architectural experience: A neurophysiological perspective on embodiment, motivation, and affordances. *Frontiers in Psychology*, *7*, Article 481. https://doi.org/10.3389/fpsyg.2016.00481

Jensen, O., & Mazaheri, A. (2010). Shaping functional architecture by oscillatory alpha activity: Gating by inhibition. *Frontiers in Human Neuroscience*, *4*, Article 186. https://doi.org/10.3389/fnhum.2010.00186

Jung, D., Kim, D. I., & Kim, N. (2023). Bringing nature into hospital architecture: Machine learning-based EEG analysis of the biophilia effect in virtual reality. *Journal of Environmental Psychology*, *89*, Article 102033. https://doi.org/10.1016/j.jenvp.2023.102033

Kawabata, H., & Zeki, S. (2004). Neural correlates of beauty. *Journal of Neurophysiology*, *91*(4), 1699–1705. https://doi.org/10.1152/jn.00696.2003

Keil, A., Debener, S., Gratton, G., Junghöfer, M., Kappenman, E. S., Luck, S. J., Luu, P., Miller, G. A., & Yee, C. M. (2014). Committee report: Publication guidelines and recommendations for studies using electroencephalography and magnetoencephalography. *Psychophysiology*, *51*(1), 1–21. https://doi.org/10.1111/psyp.12147

Klimesch, W. (1999). EEG alpha and theta oscillations reflect cognitive and memory performance: A review and analysis. *Brain Research Reviews*, *29*(2–3), 169–195. https://doi.org/10.1016/S0165-0173(98)00056-3

Klimesch, W. (2011). Evoked alpha and early access to the knowledge system: The P1 inhibition timing hypothesis. *Brain Research*, *1408*, 52–71. https://doi.org/10.1016/j.brainres.2011.06.003

Klimesch, W. (2012). Alpha-band oscillations, attention, and controlled access to stored information. *Trends in Cognitive Sciences*, *16*(12), 606–617. https://doi.org/10.1016/j.tics.2012.10.007

Knyazev, G. G. (2007). Motivation, emotion, and their inhibitory control mirrored in brain oscillations. *Neuroscience & Biobehavioral Reviews*, *31*(3), 377–395. https://doi.org/10.1016/j.neubiorev.2006.10.004

Kober, S. E., Kurzmann, J., & Neuper, C. (2012). Cortical correlate of spatial presence in 2D and 3D interactive virtual reality: An EEG study. *International Journal of Psychophysiology*, *83*(3), 365–374. https://doi.org/10.1016/j.ijpsycho.2011.12.003

Leder, H., Belke, B., Oeberst, A., & Augustin, D. (2004). A model of aesthetic appreciation and aesthetic judgments. *British Journal of Psychology*, *95*(4), 489–508. https://doi.org/10.1348/0007126042369811

Lee, S., Shin, W., & Park, E. J. (2022). Implications of neuroarchitecture for the experience of the built environment: A scoping review. *Archnet-IJAR*, *16*(2), 225–244. https://doi.org/10.1108/ARCH-09-2021-0249

Lindsen, J. P., & Bhattacharya, J. (2010). Correction of blink artifacts using independent component analysis and empirical mode decomposition. *Psychophysiology*, *47*(5), 955–955. https://doi.org/10.1111/j.1469-8986.2010.00995.x

Logothetis, N. K. (2008). What we can do and what we cannot do with fMRI. *Nature*, *453*(7197), 869–878. https://doi.org/10.1038/nature06976

Luck, S. J. (2014). *An introduction to the event-related potential technique* (2nd ed.). MIT Press.

Makeig, S., Bell, A. J., Jung, T.-P., & Sejnowski, T. J. (1996). Independent component analysis of electroencephalographic data. In D. S. Touretzky, M. C. Mozer, & M. E. Hasselmo (Eds.), *Advances in neural information processing systems* (Vol. 8, pp. 145–151). MIT Press.

Martínez-Soto, J., Gonzales-Santos, L., Pasaye, E., & Barrios, F. A. (2013). Exploration of neural correlates of restorative environment exposure through functional magnetic resonance. *Intelligent Buildings International*, *5*(sup1), 10–28. https://doi.org/10.1080/17508975.2013.807765

Michel, C. M., & Brunet, D. (2019). EEG Source imaging: A practical review of the analysis steps. *Frontiers in Neurology*, *10*, Article 325. https://doi.org/10.3389/fneur.2019.00325

Michel, C. M., Murray, M. M., Lantz, G., Gonzalez, S., Spinelli, L., & Grave de Peralta, R. (2004). EEG source imaging. *Clinical Neurophysiology*, *115*(10), 2195–2222. https://doi.org/10.1016/j.clinph.2004.06.001

Mostafavi, A., Cruz-Garza, J. G., & Kalantari, S. (2023). Enhancing lighting design through the investigation of illuminance and correlated color temperature's effects on brain activity: An EEG-VR approach. *Journal of Building Engineering*, *75*, Article 106776. https://doi.org/10.1016/j.jobe.2023.106776

Nanda, U., Pati, D., Ghamari, H., & Bajema, R. (2013). Lessons from neuroscience: Form follows function, emotions follow form. *Intelligent Buildings International*, *5*(sup1), 61–78. https://doi.org/10.1080/17508975.2013.807767

Nosek, B. A., Ebersole, C. R., DeHaven, A. C., & Mellor, D. T. (2018). The preregistration revolution. *Proceedings of the National Academy of Sciences*, *115*(11), 2600–2606. https://doi.org/10.1073/pnas.1708274114

Nunez, P. L., & Srinivasan, R. (2006). *Electric fields of the brain: The neurophysics of EEG* (2nd ed.). Oxford University Press.

Ogawa, S., Menon, R. S., Tank, D. W., Kim, S. G., Merkle, H., Ellermann, J. M., & Ugurbil, K. (1993). Functional brain mapping by blood oxygenation level-dependent contrast magnetic resonance imaging. *Biophysical Journal*, *64*(3), 803–812. https://doi.org/10.1016/S0006-3495(93)81441-3

Pascual-Marqui, R. D. (2002). Standardized low-resolution brain electromagnetic tomography (sLORETA): Technical details. *Methods and Findings in Experimental and Clinical Pharmacology*, *24*(Suppl. D), 5–12.

Pfurtscheller, G., & Lopes da Silva, F. H. (1999). Event-related EEG/MEG synchronization and desynchronization: Basic principles. *Clinical Neurophysiology*, *110*(11), 1842–1857. https://doi.org/10.1016/S1388-2457(99)00141-8

Plichta, M. M., Schwarz, A. J., Grimm, O., Morgen, K., Mier, D., Haddad, L., Gerdes, A. B., Sauer, C., Tost, H., Esslinger, C., Colman, P., Wilson, F., Kirsch, P., & Meyer-Lindenberg, A. (2012). Test-retest reliability of evoked BOLD signals from a cognitive–emotive fMRI test battery. *NeuroImage*, *60*(3), 1746–1758. https://doi.org/10.1016/j.neuroimage.2012.01.129

Rosander, K., & Von Hofsten, C. (2011). Predictive gaze shifts elicited during observed and performed actions in 10-month-old infants and adults. *Neuropsychologia*, *49*(10), 2911–2917. https://doi.org/10.1016/j.neuropsychologia.2011.06.018

Ryu, K., & Myung, R. (2005). Evaluation of mental workload with a combined measure based on physiological indices during a dual task of tracking and mental arithmetic. *International Journal of Industrial Ergonomics*, *35*(11), 991–1009. https://doi.org/10.1016/j.ergon.2005.04.005

Salinas, E., & Sejnowski, T. J. (2001). Correlated neuronal activity and the flow of neural information. *Nature Reviews Neuroscience*, *2*(8), 539–550. https://doi.org/10.1038/35086012

Shemesh, A., Leisman, G., Bar, M., & Grobman, Y. (2021). A neurocognitive study of the emotional impact of geometrical criteria of architectural space. *Architectural Science Review*, *64*(4), 394–407. https://doi.org/10.1080/00038628.2021.1940827

Shemesh, A., Leisman, G., Bar, M., & Grobman, Y. (2022). The emotional influence of different geometries in virtual spaces: A neurocognitive examination. *Journal of Environmental Psychology*, *81*, Article 101802. https://doi.org/10.1016/j.jenvp.2022.101802

Shemesh, A., Talmon, R., Karp, O., Amir, I., Bar, M., & Grobman, Y. J. (2017). Affective response to architecture—Investigating human reaction to spaces with different geometry. *Architectural Science Review*, *60*(2), 116–125. https://doi.org/10.1080/00038628.2016.1266597

Simmons, J. P., Nelson, L. D., & Simonsohn, U. (2011). False-positive psychology: Undisclosed flexibility in data collection and analysis allows presenting anything as significant. *Psychological Science*, *22*(11), 1359–1366. https://doi.org/10.1177/0956797611417632

Slobounov, S. M., Ray, W., Johnson, B., Slobounov, E., & Newell, K. M. (2015). Modulation of cortical activity in 2D versus 3D virtual reality environments: An EEG study. *International Journal of Psychophysiology*, *95*(3), 254–260. https://doi.org/10.1016/j.ijpsycho.2014.11.003

Summerfield, C., & Mangels, J. A. (2005). Coherent theta-band EEG activity predicts item-context binding during encoding. *NeuroImage*, *24*(3), 692–703. https://doi.org/10.1016/j.neuroimage.2004.09.012

Taherysayah, F., Malathouni, C., Liang, H. N., & Westermann, C. (2024). Virtual reality and electroencephalography in architectural design: A systematic review of empirical studies. *Journal of Building Engineering*, *85*, Article 108611. https://doi.org/10.1016/j.jobe.2024.108611

Vartanian, O., & Goel, V. (2004). Neuroanatomical correlates of aesthetic preference for paintings. *Neuroreport*, *15*(5), 893–897. https://doi.org/10.1097/00001756-200404090-00032

Vartanian, O., Navarrete, G., Chatterjee, A., Fich, L. B., Gonzalez-Mora, J. L., Leder, H., Modroño, C., Nadal, M., Rostrup, N., & Skov, M. (2015). Architectural design and the brain: Effects of ceiling height and perceived enclosure on beauty judgments and approach-avoidance decisions. *Journal of Environmental Psychology*, *41*, 10–18. https://doi.org/10.1016/j.jenvp.2014.11.006

Vartanian, O., Navarrete, G., Chatterjee, A., Fich, L. B., Leder, H., Modroño, C., Nadal, M., Rostrup, N., & Skov, M. (2013). Impact of contour on aesthetic judgments and approach-avoidance decisions in architecture. *Proceedings of the National Academy of Sciences*, *110*(supplement_2), 10446–10453. https://doi.org/10.1073/pnas.1301227110

Vecchiato, G., Jelic, A., Tieri, G., Maglione, A. G., De Matteis, F., & Babiloni, F. (2015). Neurophysiological correlates of embodiment and motivational factors during the perception of virtual architectural environments. *Cognitive Processing*, *16*(S1), 425–429. https://doi.org/10.1007/s10339-015-0725-6

Vecchiato, G., Tieri, G., Jelic, A., De Matteis, F., Maglione, A. G., & Babiloni, F. (2015a). Electroencephalographic correlates of sensorimotor integration and embodiment during the appreciation of virtual architectural environments. *Frontiers in Psychology*, *6*, Article 1944. https://doi.org/10.3389/fpsyg.2015.01944

Vecchiato, G., Tieri, G., Jelic, A., De Matteis, F., Maglione, A. G., & Babiloni, F. (2015b, August 25–29). *Electroencephalographic recording during immersive virtual reality: A preliminary study* [Conference session]. 2015 37th Annual International Conference of the IEEE Engineering in Medicine and Biology Society (EMBC), Milan, Italy. https://doi.org/10.1109/EMBC.2015.7318862

(*Appendix follows*)

Appendix

ERSP Plots by Aesthetic Judgment and Electrode Areas

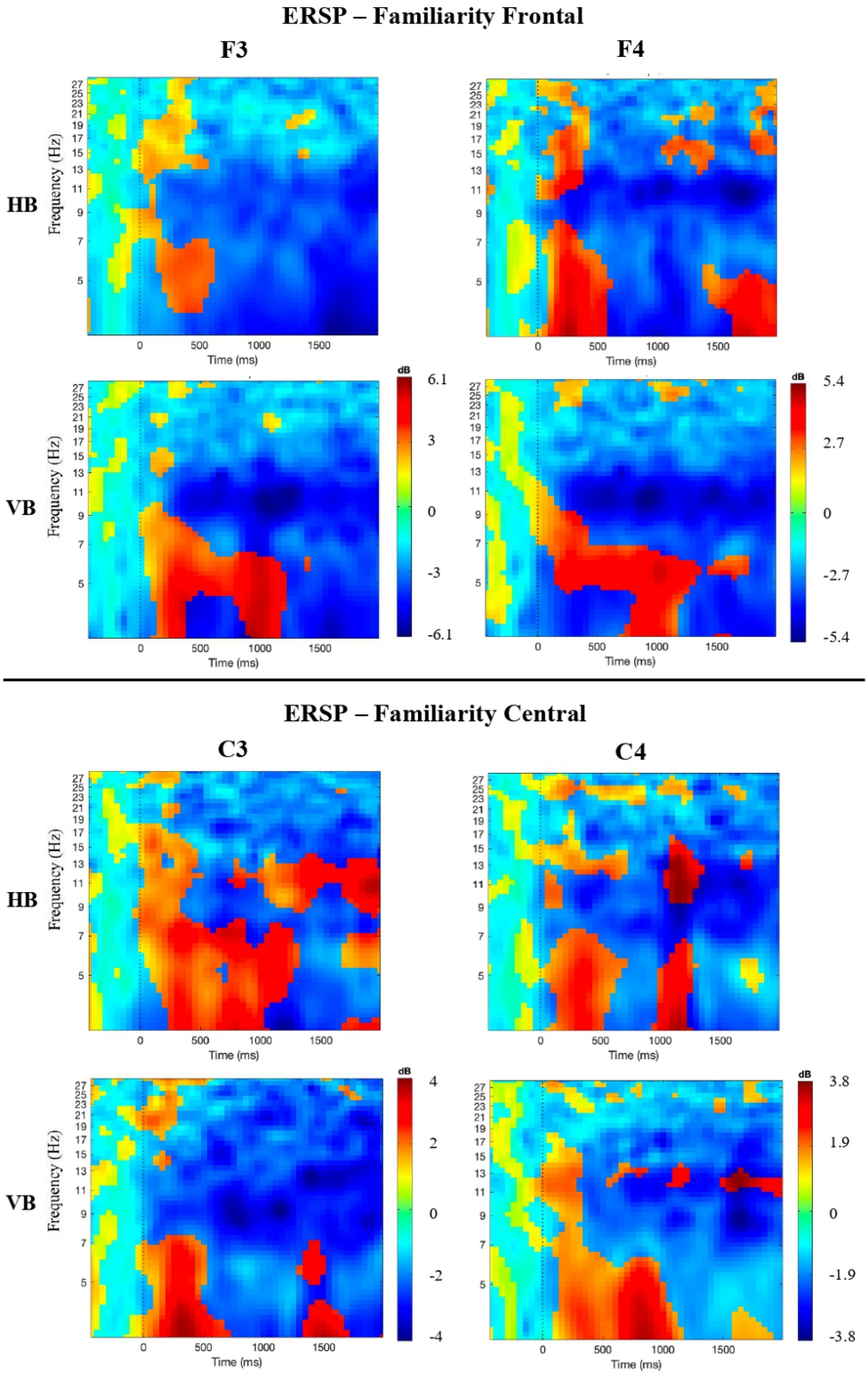

(*Appendix continues*)

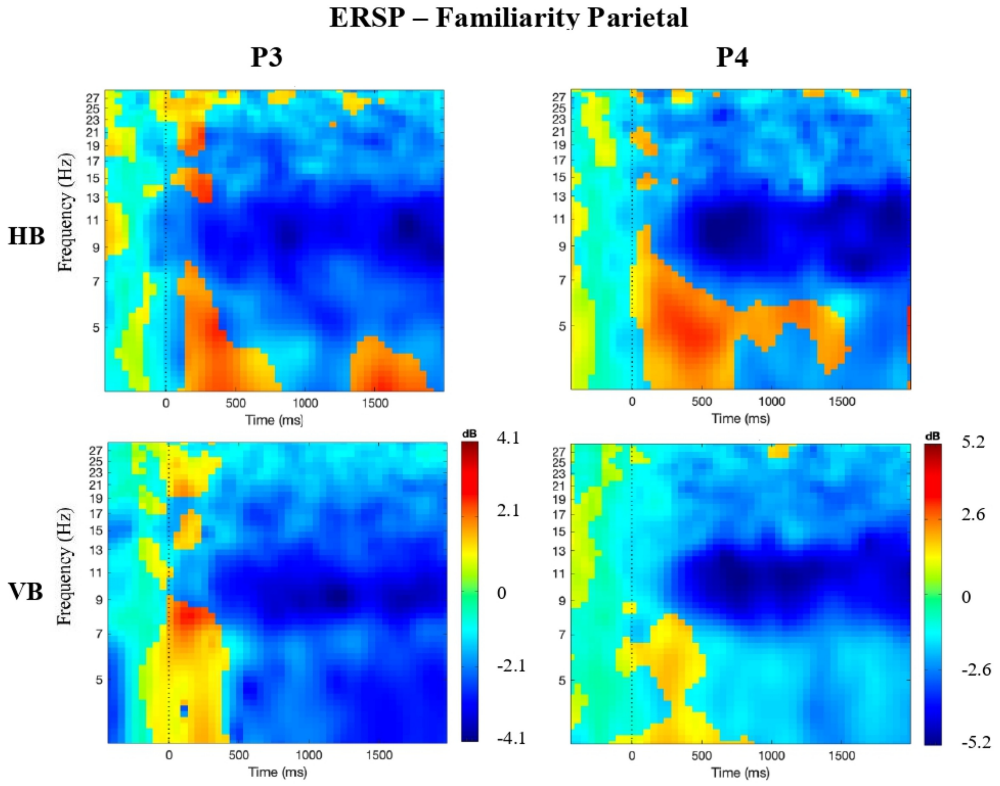

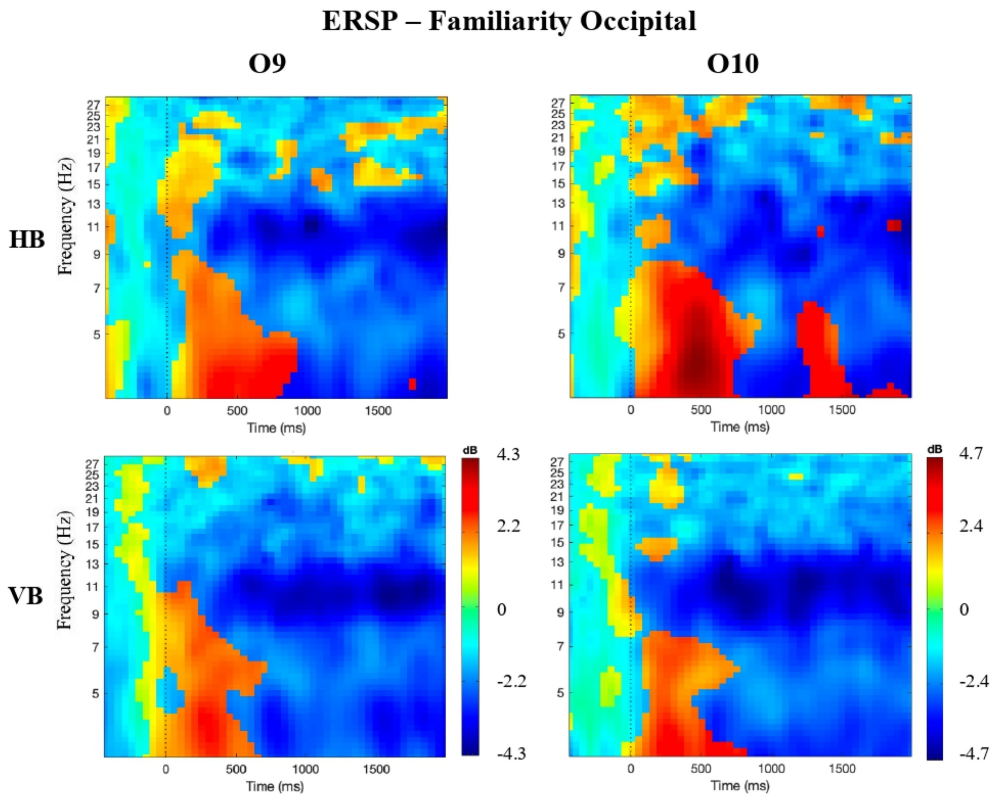

(*Appendix continues*)

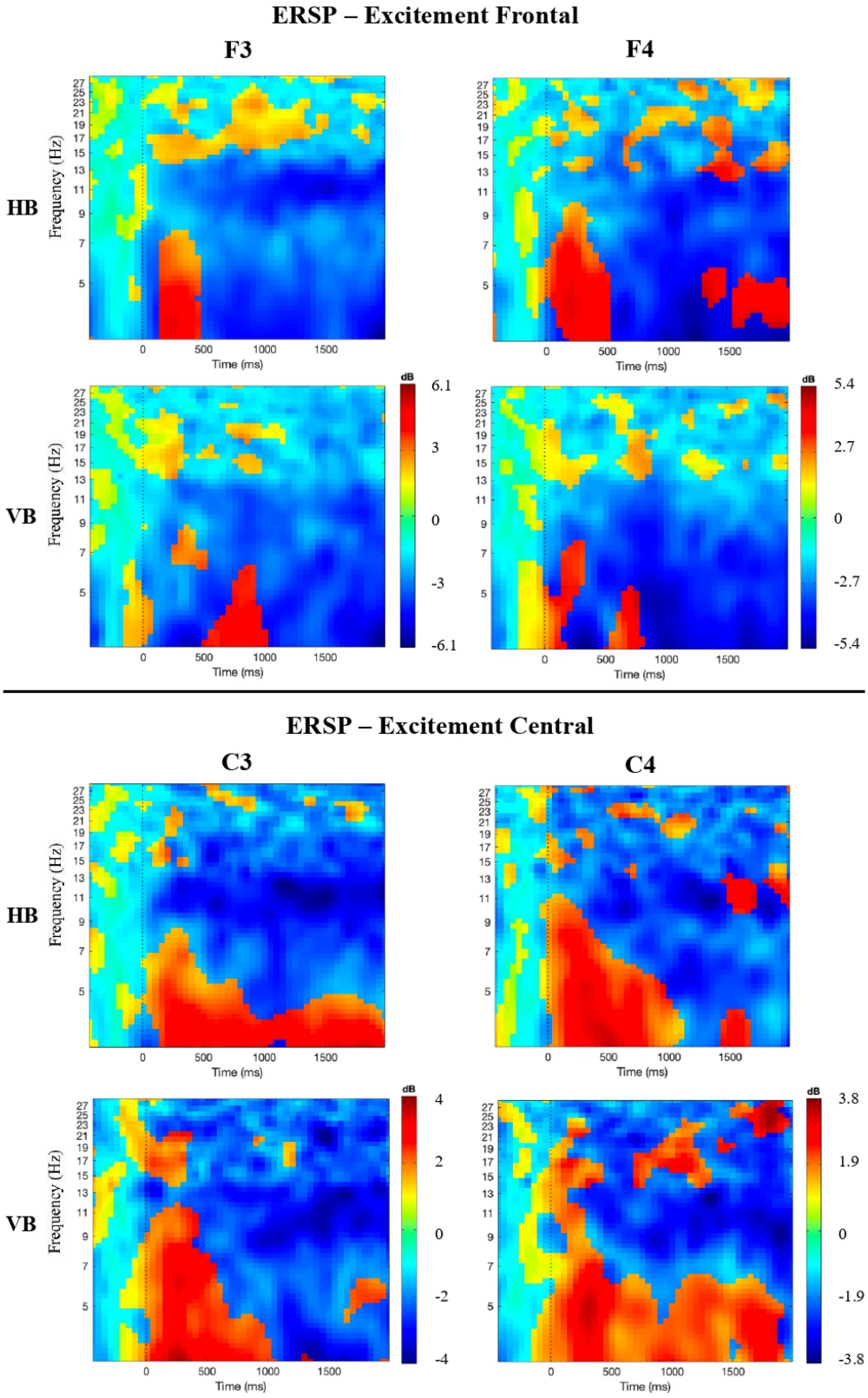

(*Appendix continues*)

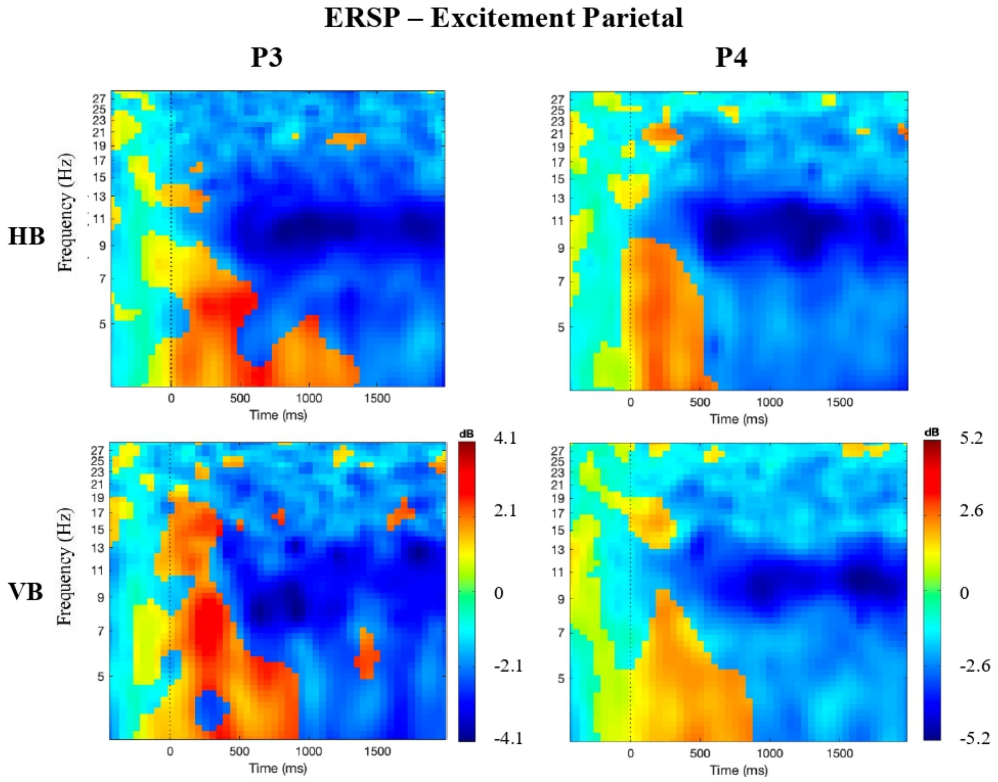

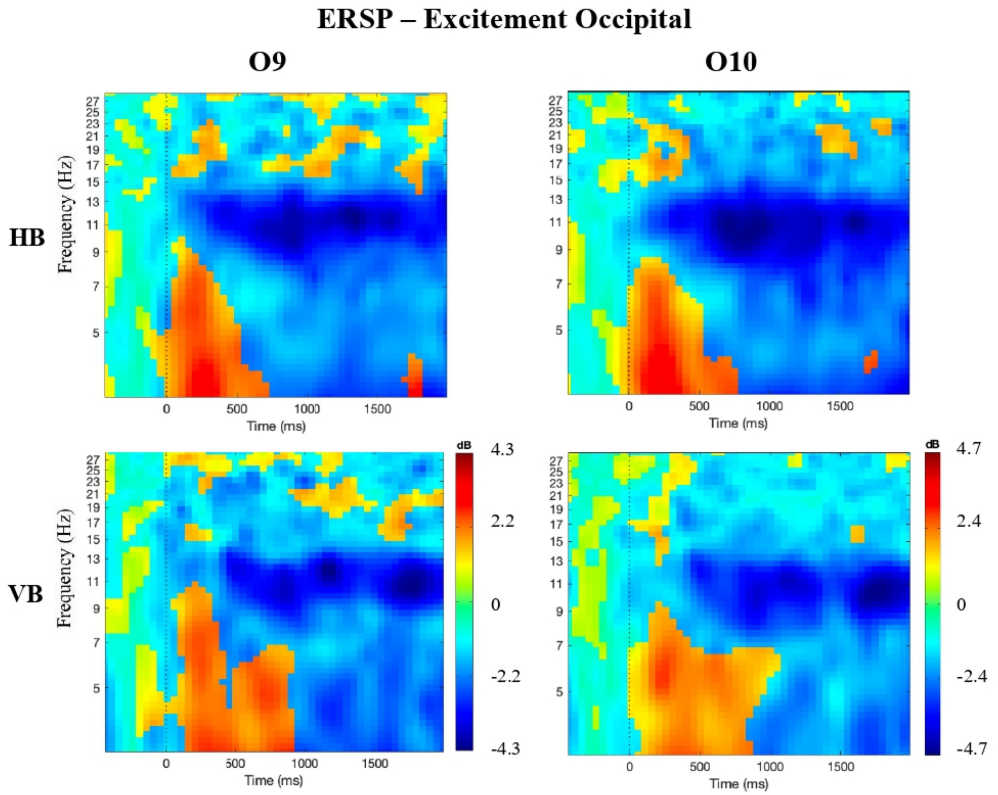

(*Appendix continues*)

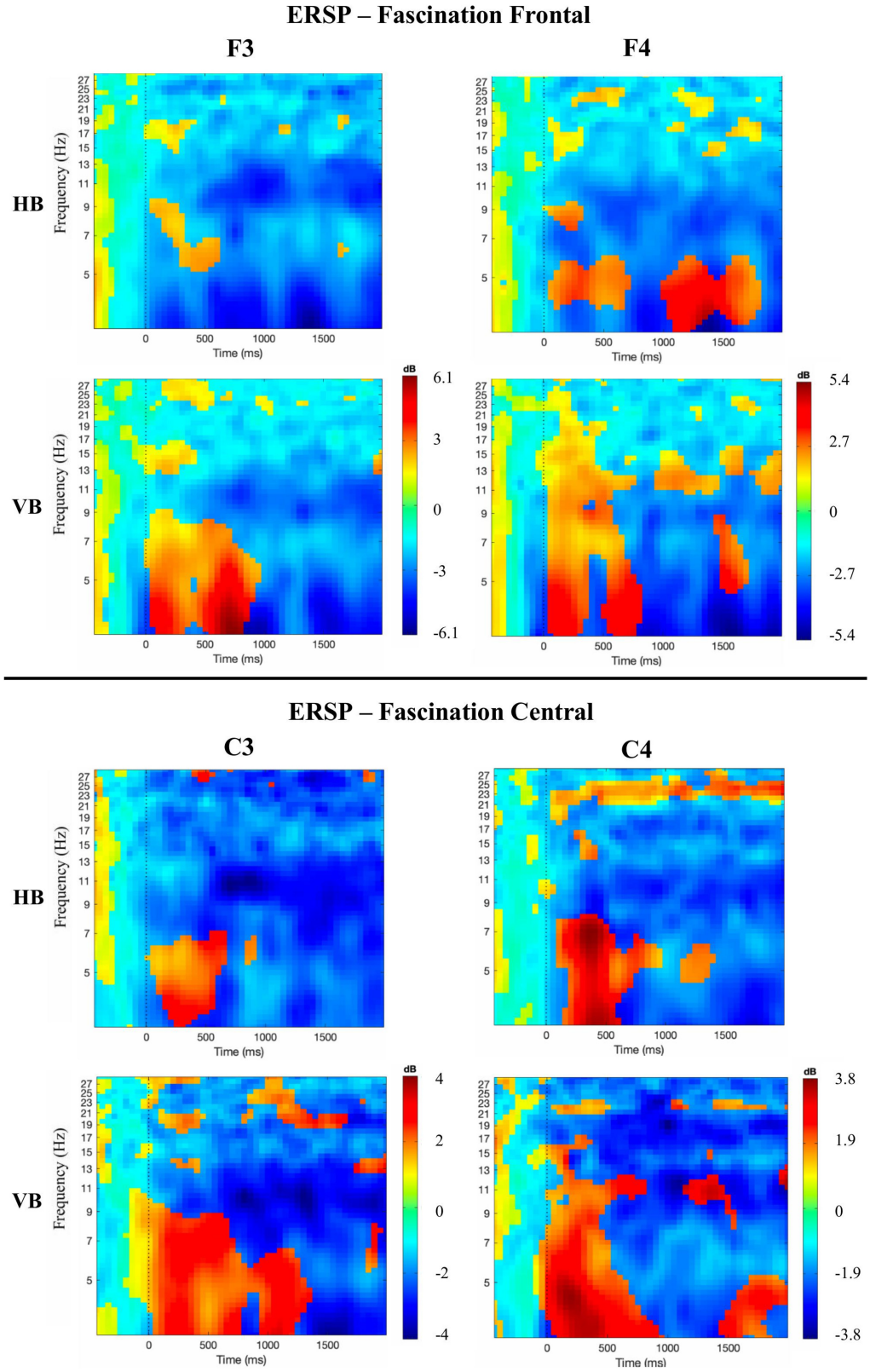

(*Appendix continues*)

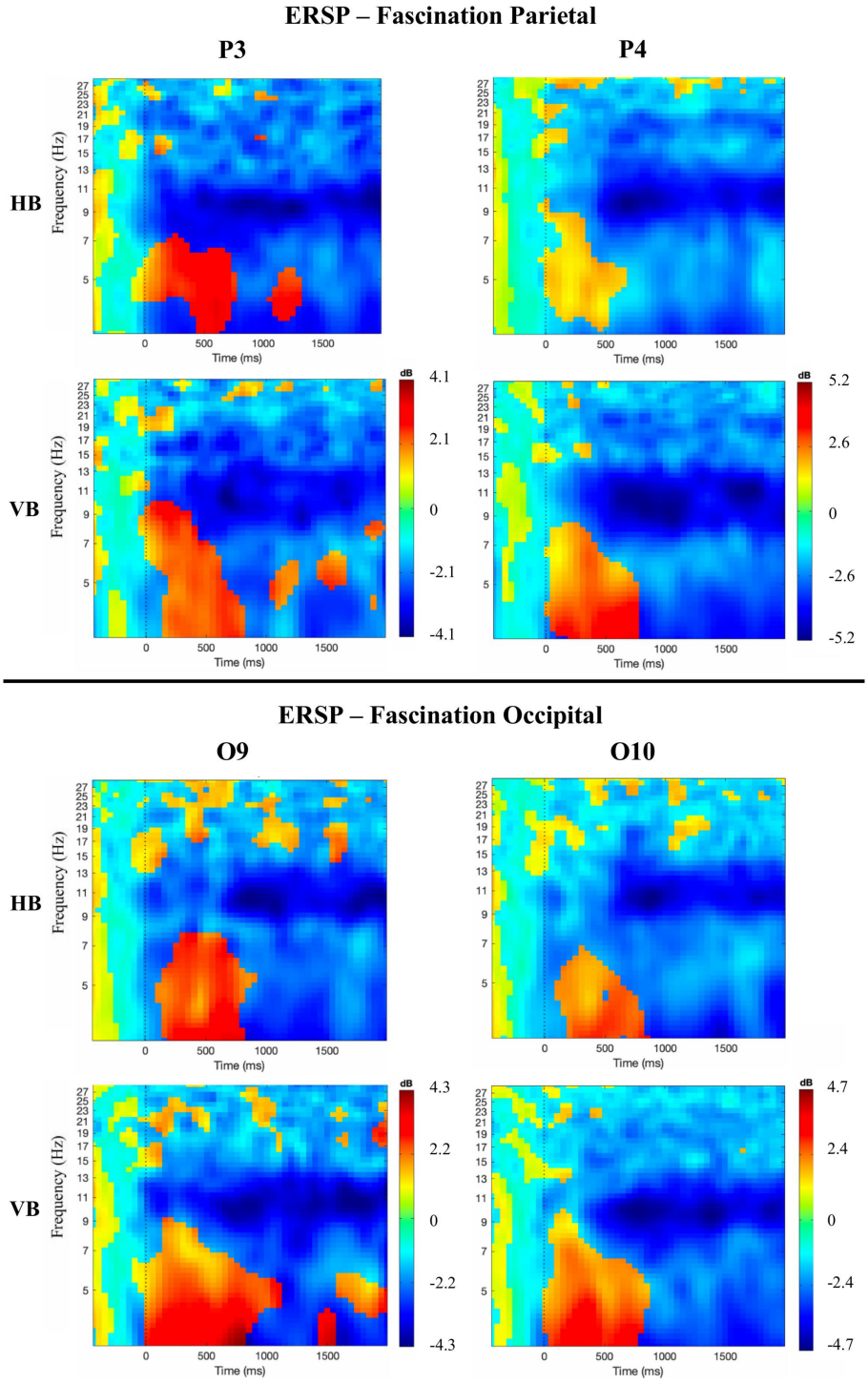

Note. ERSP = event-related spectral perturbation; HB = horizontal boundaries; VB = vertical boundaries. See the online article for the color version of this figure.

Received February 10, 2025
Revision received August 5, 2025
Accepted August 10, 2025 ■